1169

Technical Documentation

USDA-Water Erosion Prediction Project (WEPP)

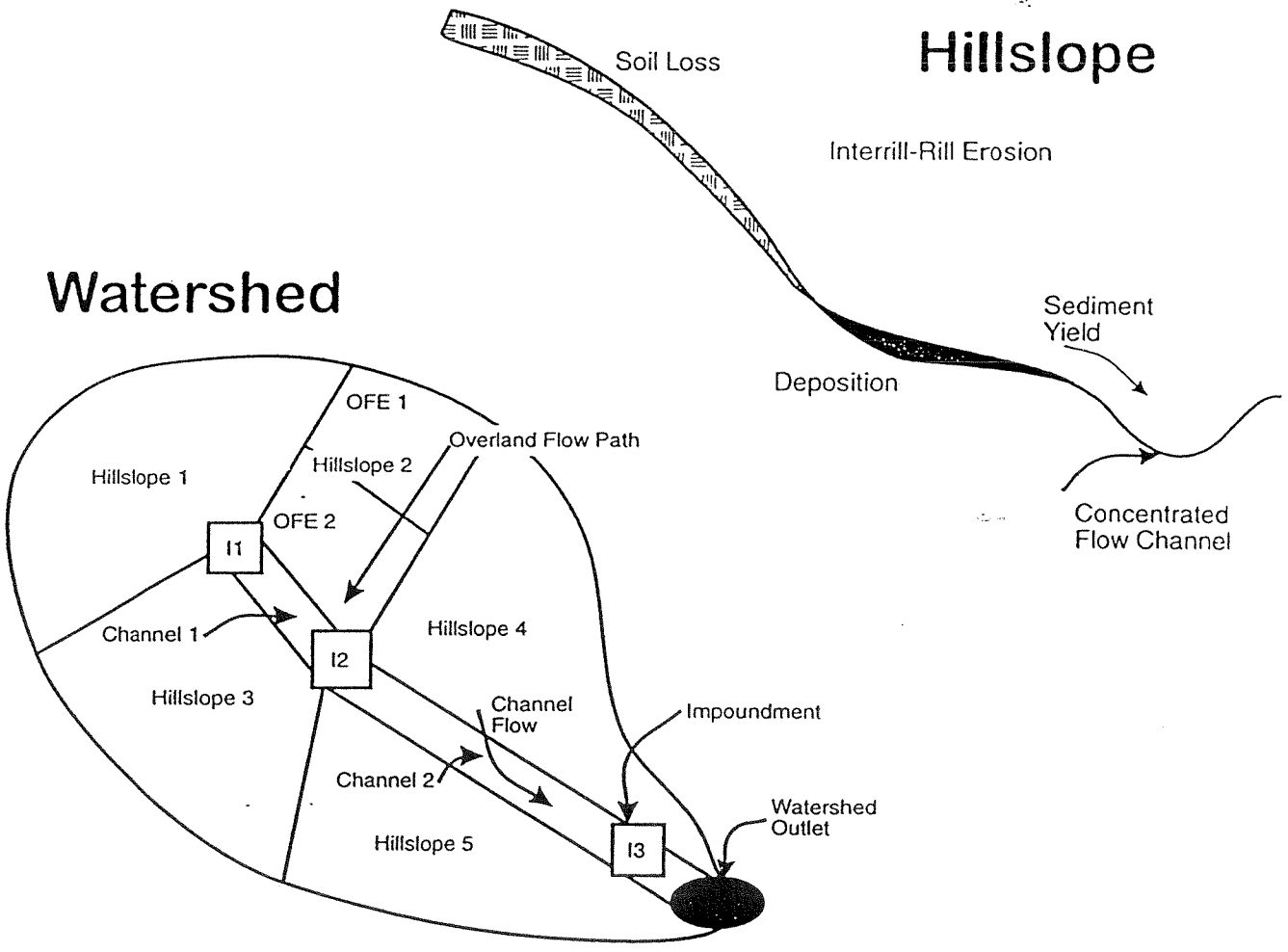

USDA - Agricultural Research Service
USDA- Natural Resource Conservation Service
USDA - Forest Service
USDI - Bureau of Land Management

NSERL Report No. 10
National Soil Erosion Research Laboratory
USDA-ARS-MWA
1196 SOIL Building
West Lafayette, IN 47907-1196

Chapter 7. SOIL COMPONENT

E.E. Alberts, M.A. Nearing, M.A. Weltz, L.M. Risse,
F.B. Pierson, X.C. Zhang, J.M. Laflen and J.R. Simanton

7.1 Introduction and Objectives

Soil properties influence the basic water erosion processes of infiltration and surface runoff, soil detachment by raindrops and concentrated flow, and sediment transport. The purpose of this chapter is to provide the WEPP user with background information on the soil and soil-related variables currently predicted in the WEPP model.

7.2 Background

7.2.1 Hydrology Parameters

Four soil variables that influence the hydrology portion of the erosion process are predicted in this component, including: 1) random roughness, 2) ridge height, 3) bulk density, and 4) effective hydraulic conductivity. Random roughness is most often associated with tillage of cropland soil, but any tillage or soil disturbing operation creates soil roughness. Ridge height, which is a form of oriented roughness, results when the soil is arranged in a regular way by a tillage implement and varies by a factor of two or more depending upon implement type. Depressional storage of rainfall and hydraulic resistance to overland flow are positively correlated with soil roughness. Soil roughness changes temporarily due to tillage, rainfall weathering, and freezing and thawing. Bulk density reflects the total pore volume of the soil and is used to predict several infiltration parameters, including wetting front suction. Bulk density changes temporally due to tillage, wetting and drying, and freezing and thawing. Adjustments to bulk density are needed to account for factors such as the volumes of entrapped air and coarse fragments in the soil.

7.2.2 Soil Detachment Parameters

Interrill erodibility (K_i) is a measure of sediment delivery rate to rills as a function of rainfall intensity and runoff rate. For cropland and rangeland soils, base K_i values were predicted from relationships developed from field experiments conducted in 1987 and 1988 (Laflen et al., 1987; Simanton et al., 1987). Base K_i values for cropland soils are measured when the soil is in a loose, unconsolidated condition typical of that found after primary and secondary tillage using conventional tillage practices. Base K_i values for rangeland are measured on undisturbed soils with all vegetation and coarse fragments removed. Base K_i values for cropland and rangeland soils need to be adjusted for factors that influence the resistance of the soil to detachment, such as live and dead root biomass, soil freezing and thawing, and mechanical and livestock compaction.

Rill erodibility (K_r) is a measure of soil susceptibility to detachment by concentrated flow, and is often defined as the increase in soil detachment per unit increase in shear stress of clear water flow. Critical shear stress (τ_c) is an important term in the rill detachment equation, and is the shear stress below which no soil detachment occurs. Critical shear stress (τ_c) is the shear intercept on a plot of detachment by clear water vs. shear stress in rills. Rate of detachment in rills may be influenced by a number of variables including soil disturbance by tillage, living root biomass, incorporated residue, soil consolidation, and freezing and thawing.

7.3 User and Climatic Inputs

The number of overland flow elements (OFEs) existing on the hillslope profile is specified by the user, with an OFE being defined as an area of uniform cropping, management, and soil characteristics.

Soil information at the mapping unit level is stored in a soil input file. If the hillslope segment begins on a ridge and ends in a alluvial valley, the location of each mapping unit can be specified and soil properties of each read into the model from the soil input file. Mapping units on the hillslope profile are specified to better predict the effects of basic soil physical and chemical properties on infiltration and soil erodibility parameters.

Because tillage is one major process altering soil properties, the user must specify information on any tillage operation that occurs during the erosion simulation. Specific inputs include: 1) implement type, 2) tillage date, 3) tillage depth, 4) surface disturbance level, and 5) residue burial amounts.

After tillage, temporal changes in soil roughness, bulk density, and hydraulic conductivity occur due to soil wetting and drying and freezing and thawing. Daily rainfall, max-min air temperatures, and soil water content are important variables in some equations that predict temporal soil properties.

7.4 Time Invariant Soil Properties

Time invariant soil properties are used to calculate baseline soil infiltration and erodibility parameters. Most baseline soil infiltration and erodibility parameters are calculated internal to the model using data read in from the soil input file (see User Summary for more information).

7.5 Random Roughness

Random roughness following a tillage operation is estimated based upon measured averages for an implement, which is similar to the approach used in EPIC (Williams et al., 1984). Table 7.5.1 shows the random roughness value assigned to each tillage implement in the current crop management input file.

RR_o and RH_o are random roughness and ridge height parameters. *RINT* represents the on-center ridge interval.

Soil random roughness immediately after a tillage operation is predicted from:

$$RR_i = RR_o\ T_{ds} + RR_{t-1}\left[1 - T_{ds}\right] \qquad [7.5.1]$$

where RR_t is the random roughness immediately after tillage (m), RR_o is the random roughness created by a tillage implement, RR_{t-1} is the random roughness of the soil surface on the day previous to the tillage operation, and T_{ds} is the fraction of the soil surface disturbed by the tillage implement. This approach accounts for the effect of prior random roughness on random roughness after tillage.

Random roughness decay with time after tillage is predicted from a modified relationship of Potter (1990):

$$RR_t = RR_i\ e^{-C_{br}\left[\frac{R_c}{b}\right]^{0.6}} \qquad [7.5.2]$$

where RR_t is the random roughness at time t (m), C_{br} is the adjustment factor for buried residue, R_c is the cumulative rainfall since tillage (m), and b is a coefficient. C_{br} is predicted by:

$$C_{br} = 1 - 0.5\ br \qquad [7.5.3]$$

where br is the mass of the buried residue in the 0-to 0.15-meter soil zone ($kg \cdot m^{-2}$). C_{br} is arbitrarily set to be no less the 0.3 in the WEPP model. The adjustment assumes that the buried residue reduces the surface roughness decay rate. The coefficient b is computed as:

Table 7.5.1. WEPP soil parameters for 78 tillage implements.

IMPLEMENT CODE & DESCRIPTION	WEPP Parameter Values				
	RR_o (m)	T_{ds}	RH_o (m)	*RINT* (m)	*TDMEAN* (m)
ANHYDISK - anhydrous applicator with closing disks	0.013	0.25	0.025	0.75	0
ANHYDROS - anhydrous applicator	0.013	0.15	0.025	0.75	0
BEDDER - bedders, lister and hippers	0.025	1	0.15	0.75	0.1
CHISCOST - chisel plow with coulters and straight chisel spikes	0.023	1	0.05	0.3	0.15
CHISCOSW - chisel plow with coulters and sweeps	0.023	1	0.05	0.3	0.15
CHISCOTW - chisel plow with coulters and twisted points or shovels	0.026	1	0.075	0.3	0.15
CHISELSW - chisel plow with sweeps	0.023	1	0.05	0.3	0.15
CHISSTSP - chisel plow, straight with spike points	0.023	1	0.05	0.3	0.15
CHISTPSH - chisel plow, twisted points or shovels	0.026	1	0.075	0.3	0.15
COMBDISK - combination tools with disks, shanks and leveling atchmnts	0.015	1	0.025	0.3	0.075
COMBSPRG - combination tools with spring teeth and rolling basket	0.015	1	0.025	0.3	0.075
CRNTFRR - drill, no-till in flat residues-ripple or bubble coulters	0.012	0.5	0.025	0.2	0
CULTFW - cultivator, row finger wheels	0.015	0.95	0.05	0.75	0.025
CULTMUSW - cultivator, row, multiple sweeps per row	0.015	0.85	0.075	0.75	0.05
CULTRD - cultivator, row, rolling disks	0.015	0.9	0.15	0.75	0.05
CULTRT - cultivator, row, ridge till	0.015	0.9	0.15	0.75	0.05
CULTSW - cultivator, row, single sweep per row	0.015	0.85	0.075	0.75	0.05
DI1WA12+ - disk, one-way with 12-16" blades	0.026	1	0.05	0.2	0.1
DI1WA18+ - disk, one-way with 18-30" blades	0.026	1	0.05	0.2	0.1
DICHSP - disk chisel plow with straight chisel spike pts	0.026	1	0.075	0.3	0.15
DICHSW - disk chisel plow with sweeps	0.023	1	0.05	0.3	0.15
DICHTW - disk chisel plow with twisted points or shovels	0.026	1	0.075	0.3	0.15
DIOFF10 - disk, offset-heavy plow > 10" spacing	0.038	1	0.05	0.2	0.1
DIOFF9 - disk, offset-primary cutting > 9" spacing	0.038	1	0.05	0.2	0.1
DIOFFFIN - disk, offset, finishing 7-9" spacing	0.038	1	0.05	0.2	0.075
DIPLOW - disk plow	0.038	1	0.05	0.2	0.1
DISGANG - disk, single gang	0.026	1	0.05	0.2	0.05
DITAF19 - disk, tandem-finishing 7-9" spacing	0.026	1	0.05	0.2	0.05
DITAHP10 - disk, tandem-heavy plowing > 10" spacing	0.026	1	0.05	0.2	0.075
DITALIAH - disk, tandem-light after harvest, before other tillage	0.026	1	0.05	0.2	0.025
DITAPR9 - disk, tandem-primary cutting > 9" spacing	0.026	1	0.05	0.2	0.075
DRDDO - drill with double disk opener	0.012	0.85	0.025	0.2	0.025
DRDF12- drill, deep furrow with 12" spacing	0.012	0.9	0.05	0.2	0.075
DRHOE - drill, hoe opener	0.012	0.8	0.05	0.2	0.025
DRNTFLSC - drill, no-till in flat residues-smooth coulters	0.012	0.4	0.025	0.2	0
DRNTFRFC - drill, no-till in flat residues-fluted coulters	0.012	0.6	0.025	0.2	0
DRNTSRFC - drill, no-till in standing stubble-fluted coulters	0.012	0.6	0.025	0.2	0
DRNTSRRI - drill, no-till in standing stubble-ripple or bubble coulters	0.012	0.5	0.025	0.2	0
DRNTSRSC - drill, no-till in standing stubble-smooth coulters	0.012	0.4	0.025	0.2	0
DRSDFP7+ - drill, semi-deep furrow or press 7-12" spacing	0.012	0.9	0.05	0.2	0.05
DRSDO - drill, single disk opener (conventional)	0.012	0.85	0.05	0.2	0.025
FCPTDP - field cultivator, primary tillage-duckfoot points	0.015	1	0.025	0.3	0.075
FCPTS12+ - field cultivator, primary tillage-sweeps 12-20"	0.015	1	0.025	0.3	0.075
FCPTSW6+ - field cultivator, primary tillage-sweeps or shovels 6-12"	0.015	1	0.025	0.3	0.075
FCSTACDP - field cultivator, secondary tillage, after duckfoot points	0.015	1	0.025	0.3	0.05

FCSTACDS - field cultivator, secondary tillage, sweeps 12-20"	0.015	1	0.025	0.3	0.05
FCSTACSH - field cultivator, secondary tillage, swp or shov 6-12"	0.015	1	0.025	0.3	0.05
FURROWD - furrow diker	0.015	0.7	0.025	0.75	0.05
HAFTT - harrow-flex-tine tooth	0.018	1	0.025	0.1	0.025
HAPR - harrow-packer roller	0.01	1	0.025	0.08	0.025
HARHCP - harrow-roller harrow (cultipacker)	0.01	1	0.025	0.08	0.025
HASP - harrow-spike tooth	0.015	1	0.025	0.05	0.025
HASPTCT - harrow-springtooth (coil tine)	0.015	1	0.025	0.05	0.025
MANUAPPL - applicator, subsurface manure	0.013	0.4	0.025	0.75	0
MOPL - plow, moldboard, 8"	0.043	0.1	0.05	0.4	0.15
MOPLUF - plow, moldboard with uphill furrow (Pacific NW only)	0.043	1	0.05	0.4	0.15
MULCHT - mulch treader	0.015	1	0.025	0.05	0.025
PARAPLOW - paratill/paraplow	0.01	0.3	0.025	0.36	0.2
PLDDO - planter, double disk openers	0.012	0.15	0.025	0.75	0.05
PLNTFC - planter, no-till with fluted coulters	0.012	0.15	0.025	0.75	0
PLNTRC - planter, no-till with ripple coulters	0.012	0.15	0.025	0.75	0
PLNTSC - planter, no-till with smooth coulters	0.012	0.15	0.025	0.75	0
PLRO - planter, runner openers	0.013	0.2	0.025	0.75	0.05
PLRT - planter, ridge-till	0.013	0.4	0.1	0.75	0.05
PLSDDO - planter, staggered double disk openers	0.013	0.15	0.025	0.75	0.05
PLST2C - planter, strip-till with 2 or 3 fluted coulters	0.013	0.3	0.025	0.75	0.05
PLSTRC - planter, strip-till with row cleaning devices (8-14" wide)	0.013	0.4	0.025	0.75	0.05
RORRP - rodweeder, plain rotary rod	0.01	1	0.025	0.13	0.05
RORRSC - rodweeder, rotary rod with semi-chisels or shovels	0.01	1	0.025	0.13	0.05
ROTHOE - rotary hoe	0.012	1	0	0	0.025
ROTILPO - rotary tiller-primary operation 6" deep	0.015	1	0	0	0.15
ROTILSO - rotary tiller-secondary operation 3" deep	0.015	1	0	0	0.075
ROTILST - rotary tiller, strip tillage - 12" tilled on 40" rows	0.015	0.3	0	0	0.075
SUBCC - subsoil-chisel, combination chisel	0.015	1	0.075	0.3	0.4
SUBCD - subsoiler, combination disk	0.015	1	0.075	0.3	0.4
SUBVRIP - subsoiler, V ripper 20" spacing	0.015	0.2	0.075	0.5	0.4
UNSMWBL - undercutter, stubble-mulch sweep (20-30"wide) or blade	0.015	1	0.075	1	0.075
UNSMWBP - undercutter, stubble-mulch sweep or blade plows > 30" wide	0.015	1	0.075	1.5	0.075

$$b = 63 + 62.7 \ln(50\ orgmat) + 1570\ clay - 2500\ clay^2 \quad [7.5.4]$$

where *orgmat* is the soil organic matter content (0-1), and *clay* is the soil clay content (0-1). Only the C_{br} coefficient and its associated equation were added to the Potter (1990) equation.

Since WEPP assumes that surface roughness in a rill is relatively small and is also independent of roughness in interrill, friction due to form roughness is not included in the total friction factor of the rill. This is reasonable only after the rill has formed. But during rill initiation stage, surface roughness should be considered. It is expected that rill formation should be slower on a rougher surface than on a smoother one. This can be realized by relating critical shear (τ_c) to *RR*, because WEPP assumes that rill erosion will not be initiated until flow shear exceeds the critical shear. By calibration, the following equation was obtained:

$$C\tau_{rr} = 1.0 + 8.0\ (RR_t - 0.006) \quad [7.5.5]$$

where $C\tau_{rr}$ is the adjustment factor, and 0.006 is the minimum *RR* value in meters. τ_c is multiplied by $C\tau_{rr}$, thus τ_c increases as *RR* increases, which reduces rill detachment.

Table 7.5.1 contains the recommended values for five tillage parameters - RR_o (random roughness) immediately after tillage, T_{ds} (fraction of soil surface disturbed by the tillage implement), RH_o (ridge height immediately after tillage), *RINT* (ridge interval), and *TDMEAN* (the mean tillage depth associated with each implement). See Chapter 9 for information on tillage implement effects on residue burial.

7.6 Ridge Height

A ridge height value is assigned to a tillage implement based upon measured averages for each implement (see Table 7.5.1 for assigned ridge height values), which is similar to the approach used in EPIC (Williams et al., 1984).

Ridge height decay following tillage is predicted from:

$$RH_t = RH_o \, e^{-C_{br}\left[\frac{R_c}{b}\right]^{0.6}} \qquad [7.6.1]$$

where RH_t is the ridge height (m) at time t, RH_o is the ridge height immediately after tillage (m), and C_{br}, R_c, and b are as defined in section 7.5.

Large ridges made by a ridging cultivator or a similar ridging implement do not decay as fast as smaller ridges made by a disk or chisel plow. Criteria used to identify a well-defined ridge-furrow system is that ridge height after tillage for any implement in the tillage sequence is ≥ 0.1 m and the ridge interval is between 0.6 and 1.4 meters. For this condition, ridge height is not allowed to decay below 0.1 m.

7.7 Bulk Density

7.7.1 Tillage Effects

Soil bulk density changes are used to predict changes in infiltration parameters. Bulk density after tillage is difficult to predict because of limited knowledge, particularly for point- and rolling-type implements, of how an implement interacts with a soil as influenced by tillage speed, tillage depth, and soil cohesion.

The approach chosen to account for the influence of tillage on soil bulk density is to use a classification scheme where each implement is assigned a tillage disturbance value from 0 to 1, which is similar to the approach used in EPIC (Williams et al., 1984). The concept is based, in part, on measured effects of various tillage implements on residue cover (see tillage intensity values in Chapter 9).

The equation used to predict soil bulk density after tillage is (Williams et al., 1984):

$$\rho_t = \rho_{t-1} - \left[\left(\rho_{t-1} - 0.667\,\rho_c\right) T_{ds}\right] \qquad [7.7.1]$$

where ρ_t is the bulk density after tillage ($kg \cdot m^{-3}$), ρ_{t-1} is the bulk density before tillage ($kg \cdot m^{-3}$), ρ_c is the consolidated soil bulk density ($kg \cdot m^{-3}$) at 0.033 *MPa* of tension, and T_{ds} is the fraction of the soil surface disturbed by the tillage implement (0-1).

Consolidated soil bulk density, ρ_c, is calculated by the model from the soil input data from the relationship:

$$\rho_c = (1.514 + 0.25\,sand - 13.0\,sand\,orgmat - 6.0\,clay\,orgmat - 0.48\,clay\,CEC_r)\,10^3 \qquad [7.7.2]$$

where ρ_c is the consolidated soil bulk density ($kg \cdot m^{-3}$) at 0.033 *MPa* of tension, *sand* is the sand content (0-1), *orgmat* is the organic matter content (0-1), *clay* is the clay content (0-1), and CEC_r is the ratio of the cation exchange capacity of the clay (CEC_c) to the clay content of the soil.

The cation exchange capacity of the clay fraction of the soil is calculated from:

$$CEC_c = CEC - orgmat\ (142 + 170\ D_g) \quad [7.7.3]$$

where CEC is the cation exchange capacity of the soil ($meq/100g$) and D_g is the average depth of the horizon of interest (m).

The WEPP model currently assumes the depth of primary tillage to be 0.2 meters and the depth of secondary tillage to be 0.1 meters. The model uses the information in the soil input file to create a new set of soil layers which are appropriate for use in the infiltration and percolation computations. The top soil layer has a thickness of 0.1 meters, and the second soil layer also has a thickness of 0.1 meters. All remaining soil layers to a total maximum possible depth of 1.8 meters have a thickness of 0.2 meters. Soil properties for the newly-created layers are obtained by using weighted averages of input soil properties from the corresponding depths. All processes that influence soil bulk density are modeled within the primary and secondary tillage zones.

7.7.2 Soil Water Content Effects

The bulk density of the soil at the wilting point, ρ_d, is predicted from:

$$\rho_d = \left[-0.024 + 0.001\ \rho_c + 1.55\ clay\ CEC_r + clay^2\ CEC_r^2 - 1.1\ CEC_r^2\ clay - 1.4\ orgmat\right] 10^3 \quad [7.7.4]$$

The residual water content of the soil is predicted from (Baumer, personal communication):

$$\theta_r = (0.000002 + 0.0001\ orgmat + 0.00025\ clay\ CEC_r^{0.45})\ \rho_t \quad [7.7.5]$$

where θ_r is the residual volumetric water content of the soil ($m^3 \cdot m^{-3}$).

The volumetric water content at 0.033 MPa of tension (field capacity), θ_{fc}, is predicted from:

$$\theta_{fc} = 0.2391 - 0.19\ sand + 2.1\ orgmat + 0.72\ \theta_d \quad [7.7.6]$$

The volumetric water content at 1.5 MPa of tension (wilting point), θ_d, is predicted from:

$$\theta_d = 0.0022 + 0.383\ clay - 0.5\ clay^2\ sand^2 + 0.265\ clay\ CEC_r^2 - (0.06\ clay^2 + 0.108\ clay)\left[\frac{\rho_t}{1000}\right]^2 \quad [7.7.7]$$

7.7.3 Rainfall Consolidation

Rainfall on freshly-tilled soil consolidates it and increases soil bulk density. Soil bulk density increases by rainfall are predicted from (Onstad et al., 1984):

$$\rho_d = \rho_t + \Delta\ \rho_{rf} \quad [7.7.8]$$

where ρ_d is the bulk density after rainfall ($kg \cdot m^{-3}$), ρ_t is the bulk density after tillage ($kg \cdot m^{-3}$), and $\Delta\rho_{rf}$ is the bulk density increase due to consolidation by rainfall ($kg \cdot m^{-3}$).

The increase in soil bulk density from rainfall consolidation ($\Delta\rho_{rf}$) is calculated from:

$$\Delta\ \rho_{rf} = \Delta\ \rho_{mx}\ \frac{R_c}{0.01 + R_c} \quad [7.7.9]$$

where $\Delta\rho_{mx}$ is the maximum increase in soil bulk density with rainfall and R_c is the cumulative rainfall since tillage (m).

The maximum increase in soil bulk density with rainfall is predicted from:

$$\Delta\rho_{mx} = 1650 - 2900\ clay + 3000\ clay^2 - 0.92\ \rho_t \qquad [7.7.10]$$

and if $\Delta\rho_{mx}$ is ≤ 0.0, then $\Delta\rho_{mx} = 0.0$.

The upper boundary for soil bulk density change with rainfall is reached after a freshly-tilled soil receives 0.1 m of rainfall.

7.7.4 Weathering Consolidation

For most soils, 0.1 m of rainfall does not fully consolidate the soil. Consolidated soil bulk density (ρ_c) is assumed to be the upper boundary to which a soil naturally tends to consolidate.

The difference between the naturally consolidated bulk density and the bulk density after 0.1 m of rainfall is:

$$\Delta\rho_c = \rho_c - \rho_t \qquad [7.7.11]$$

where $\Delta\rho_c$ is the difference in soil bulk density between a soil that is naturally consolidated and one that has received 0.1 m of rainfall. ρ_t is soil bulk density on the day cumulative rainfall since tillage equals 0.1 m.

The adjustment for increasing bulk density due to weathering and longer-term soil consolidation is computed from:

$$\Delta\rho_{wt} = \Delta\rho_c\ F_{dc} \qquad [7.7.12]$$

where $\Delta\rho_{wt}$ is the daily increase in soil bulk density ($kg \cdot m^{-3}$) after 0.1 m of rainfall, and F_{dc} is the daily consolidation factor.

The daily bulk density consolidation factor is predicted from:

$$F_{dc} = 1 - e^{-0.005\ daycnt} \qquad [7.7.13]$$

where *daycnt* is a counter to keep track of the number of days since the last tillage operation.

Soil bulk density changes following tillage are predicted from:

$$\rho_t = \rho_{t-1} + \Delta\rho_{rf} + \Delta\rho_{wt} \qquad [7.7.14]$$

where the tillage occurred the previous day ($t-1$) and the variables have been previously described.

7.8 Porosity

Total soil porosity (ϕ_t) is predicted from soil bulk density by:

$$\phi_t = 1 - \rho_t/2650 \qquad [7.8.1]$$

where ρ_t is the bulk density ($kg \cdot m^{-3}$) at time t.

The volume of entrapped air in the soil (F_a) is calculated from (Baumer, personal communication):

$$F_a = 1.0 - \frac{3.8 + 1.9\ clay^2 - 3.365\ sand + 12.6\ CEC_r\ clay + 100\ orgmat\ (sand/2)^2}{100} \quad [7.8.2]$$

where the clay, sand, and organic matter contents of the soil are given as a fraction (0-1).

The correction for the volume of coarse fragments in the soil (F_{cf}) is predicted from (Brakensiek et al., 1986):

$$F_{cf} = 1 - V_{cf} \quad [7.8.3]$$

V_{cf} is the fraction of coarse fragments by volume (0-1) and is predicted from:

$$V_{cf} = \frac{M_{cf}\frac{\rho_t}{1000}}{2.65\left(1 - M_{cf}\right)} \quad [7.8.4]$$

where M_{cf} is the fraction of coarse fragments by weight (0-1).

The effective porosity of the soil (ϕ_e) is calculated from the total porosity determined from soil bulk density (< 2-mm material) and adjusted for the volume of coarse fragments and the volume of entrapped air. ϕ_e is computed from:

$$\phi_e = \phi_t\ F_a\ F_{cf} \quad [7.8.5]$$

Volumetric soil water contents at 0.020, 0.033, and 1.5 *MPa* are adjusted for the volumes of entrapped air (F_a) and coarse fragments (F_{cf}). The adjusted soil parameters are then used in soil water storage computations (see Chapter 5).

7.9 Infiltration Parameters for the WEPP Green-Ampt Model

The key parameter for the WEPP model in terms of infiltration is the Green-Ampt effective hydraulic conductivity (K_e). This parameter is related to the saturated conductivity of the soil, but it is important to note that it is not the same as or equal in value to the saturated conductivity of the soil. The second soil-related parameter in the Green-Ampt model is the wetting front matric potential term. That term is calculated internal to WEPP as a function of soil type, soil water content, and soil bulk density: it is not an input variable.

The effective conductivity value for the soil may be input into the third numerical data line of the soil data file, immediately after the inputs for soil erodibility. If the user does not know the effective conductivity of the soil, he/she may insert a zero and the model will calculate a value based on the equations presented here for the time-variable case.

The model will run in two modes by either: A) using a "baseline" effective conductivity (K_b) which the model automatically adjusts within the continuous simulation calculations as a function of soil management and plant characteristics, or B) using a constant input value of K_{ec}. The second numerical data line of the soil file contains a flag (0 or 1) which the model uses to distinguish between these two modes. A value of 1 indicates that the model is expecting the user to input a K_b value which is a function of soil only, and which will be internally adjusted to account for management practices. A value of 0 indicates the model is expecting the user to input a value of K_{ec} which will not be internally adjusted and must therefore be representative of both the soil and the management practice being modeled. It is essential that the flag (0 or 1) be set consistently with the input value of effective conductivity for the upper soil layer.

7.9.1 Cropland Temporally-varying Case: 'Baseline' Effective Conductivity

Values for "baseline" effective conductivity (K_b) may be estimated using the following equations:

$$K_b = -0.265 + 0.0086\,(100\,sand)^{1.8} + 11.46\,CEC^{-0.75} \qquad [7.9.1]$$

for soils with =< 40% clay content; and

$$K_b = 0.0066e^{\left[\frac{2.44}{clay}\right]} \qquad [7.9.2]$$

for soils with > 40% clay content. In these equations, *sand* and *clay* are the fractions of sand and clay, and *CEC* (*meq*/100*g*) is the cation exchange capacity of the soil. In order for these equations to work properly, the input value for cation exchange capacity should always be greater than 1 *meq*/100*g*. These equations were derived based on model optimization runs to measured and curve number (fallow condition) runoff amounts. Forty three soil input files were used to develop the relationships. Table 7.9.1 shows the results of the optimization and the estimated values of K_b. Figure 7.9.1 is a plot of optimized vs. estimated K_b for the 43 soils. Table 7.9.2 shows the results of comparisons to measured natural runoff plot data from 11 sites.

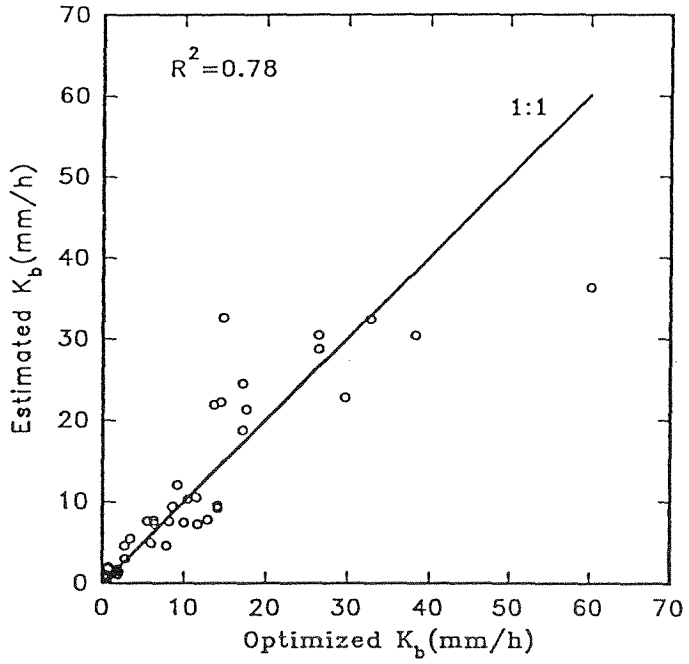

Figure 7.9.1. Estimated values of baseline hydraulic conductivity for the time-variable case plotted against those calibrated from curve number predictions.

Table 7.9.1. Optimized and estimated effective hydraulic conductivity values for the case of constant effective conductivity for fallow soil, K_{ef} and baseline K_b.

Soil	Sand Content (%)	Clay Content (%)	Organic Matter Content (%)	CEC ($meq/100g$)	Simulator Measured K_e ($mm \cdot h^{-1}$)	Opt. Constant K_{ef} ($mm \cdot h^{-1}$)	Est. Constant K_{ef} ($mm \cdot h^{-1}$)	Opt. Baseline K_b ($mm \cdot h^{-1}$)	Est. Baseline K_b ($mm \cdot h^{-1}$)
Sharpsburg	5.2	40.1	2.8	29.4	7.3	1.6	1.8	1.8	1.8
Hersh	72.3	10.9	1.1	7.7	15.8	6.5	6.4	17.6	21.3
Keith	48.9	19.3	1.5	18.3	3.5	4.7	4.8	11.5	10.5
Amarillo	85.0	7.3	0.3	5.1	15.0	7.0	7.3	26.6	28.7
Woodward	51.7	13.0	2.2	11.6	12.0	4.5	4.9	9.2	12.0
Heiden	8.6	53.1	2.2	33.3	4.7	0.3	0.3	0.34	0.45
Los Banos	15.5	43.7	2.0	39.1	3.9	0.8	1.0	1.1	1.1
Portneuf	19.5	11.1	1.2	12.6	7.9	2.0	2.5	2.7	3.0
Nansene	20.1	12.8	1.9	16.6	5.3	2.2	2.6	2.8	3.0
Palouse	9.8	20.1	2.6	19.6	2.6	1.8	1.9	2.0	1.5
Zahl	46.3	24.0	2.5	19.5	5.7	5.0	4.5	14.1	9.5
Pierre	16.9	49.5	2.7	35.7	2.4	0.4	0.3	0.71	0.61
Williams	40.8	26.9	2.6	22.7	8.3	4.4	4.1	12.9	7.7
BarnesND	39.3	26.5	3.9	23.2	16.7	4.4	4.0	11.7	7.2
Sverdrup	75.3	7.9	2.0	11.0	20.3	6.3	6.6	14.5	22.2
BarnesMN	48.6	17.0	3.2	19.5	19.1	4.7	4.7	10.4	10.3
Mexico	5.5	25.3	2.5	21.3	6.2	0.3	0.3	0.34	1.1
Grenada	1.8	20.2	1.8	11.8	3.4	0.6	0.6	0.7	1.6
Tifton	86.4	2.8	0.7	2.1	14.9	6.6	7.4	14.8	32.6
Bonifay	91.2	3.3	0.5	1.7	34.8	14.8	14.2	60.2	36.4
Cecil	69.9	11.5	0.7	2.0	13.3	7.4	6.0	17.2	24.4
Hiwassee	63.7	14.7	1.3	4.4	13.6	6.3	5.8	17.2	18.7
Gaston	37.2	37.9	1.7	9.2	3.6	1.8	1.7	6.3	7.7
Opequon	37.7	31.1	2.3	12.9	7.6	1.9	1.7	6.3	7.3
Frederick	25.1	16.6	2.1	8.2	2.9	2.7	3.0	5.9	4.9
Manor	44.0	25.2	2.5	13.2	10.0	4.6	4.3	14.1	9.2
Collamer	6.0	15.0	1.7	9.2	3.6	0.7	0.7	0.73	2.1
Miamian	31.3	25.9	2.4	14.9	4.4	1.4	1.5	3.3	5.5
Lewisburg	38.5	29.3	1.4	12.5	3.7	1.8	1.8	5.5	7.6
Miami	4.2	23.1	1.3	13.3	0.9	1.6	1.5	1.7	1.5
Colonie	90.5	2.1	0.1	10.0		14.5	14.2	38.3	30.4
Pratt	89.0	2.2	0.4	3.1		13.3	14.2	32.8	32.4
Shelby	27.8	29.0	3.0	16.5		2.9	3.2	7.8	4.6
Monona	7.1	23.5	2.0	20.1		1.7	1.7	1.9	1.2
Ontario	44.2	14.9	4.5	11.8		4.2	4.4	8.6	9.4
Stephensville	73.2	7.9	1.6	7.2		6.2	6.4	13.7	21.9
Providence	2.0	19.8	0.8	9.3		0.7	0.6	0.7	1.9
Egan	7.0	32.2	3.7	25.1		1.7	1.7	1.8	1.0
Barnes	39.4	23.2	3.4	18.4		4.1	4.0	10.0	7.4
Thatuna	28.0	23.0	4.3	16.2		1.3	1.4	2.6	4.6
Caribou	38.8	13.7	3.8	13.2		4.3	4.0	8.2	7.6
Tifton	87.0	5.7	0.7	4.1		7.2	7.4	26.6	30.4
Cecil	66.5	19.6	0.9	4.8		6.3	6.2	29.7	22.8

Table 7.9.2. WEPP estimated runoff in terms of: A) model efficiency on a storm-by-storm basis and B) average annual runoff.

A. Comparison of model efficiency

Site	Number of Years	Number of Events	Model Efficiency		
			WEPP Opt. K_b	*CN*	WEPP Est. K_b
Bethany, MO	10	109	0.82	0.72	0.81
Castana, IA	12	90	0.48	0.10	0.12
Geneva, NY	10	97	0.73	0.58	0.62
Guthrie, OK	15	170	0.86	0.77	0.85
Holly Springs, MS	8	208	0.87	0.79	0.69
Madison, SD	10	60	0.77	0.69	0.74
Morris, MN	11	72	0.59	-1.06	-0.21
Pendleton, OR	11	82	0.06	-0.33	-0.69
Presque Isle, ME	9	99	0.45	-0.25	0.32
Tifton, GA	7	64	0.67	0.24	0.59
Watkinsville, GA	6	110	0.84	0.74	0.84

B. Comparison of average annual runoff

Site	Number of Years	Average Annual Rainfall	Average Annual Runoff		
			Measured	CN	WEPP
		mm	----------*mm*----------		
Bethany, MO	10	754	222	175	205
Castana, IA	12	747	102*	125	148
Geneva, NY	10	828	168*	79	110
Guthrie, OK	15	745	154	78	121
Holly Springs, MS	8	1328	557	216	299
Madison, SD	10	577	56*	69	65
Morris, MN	11	604	40*	33	75
Pendleton, OR**	11	595	71	60	27
Presque Isle, ME	9	846	107*	89	47
Tifton, GA	7	1227	289	135	171
Watkinsville, GA	6	1445	431	395	392

* indicates winter runoff not measured.

** Pendleton did not have any events with less than 80 mm of rainfall since last tillage.

Model efficiency is a quantification of how well the model predicted runoff on an individual storm basis. At each of the eleven sites the model predicted runoff better on a storm-by-storm basis using the estimated K_b values (Eqs. [7.9.1] and [7.9.2]) than did the curve number approach. For purposes of erosion prediction it is more important to predict the individual storms accurately than to predict the total annual runoff volume, because it is a relatively small number of intense storms which cause most of the erosion.

Physically, the K_b value should approximate the value of K_e for the first storm after tillage on a fallow plot of land. Figure 7.9.2 shows a plot of the optimized K_b versus a measurement of K_b obtained using the data from the WEPP erodibility sites under a rainfall simulator. These values are also listed in Table 7.9.2. In general, the rainfall simulator measured K_b values tended to be greater than the corresponding optimum K_b values.

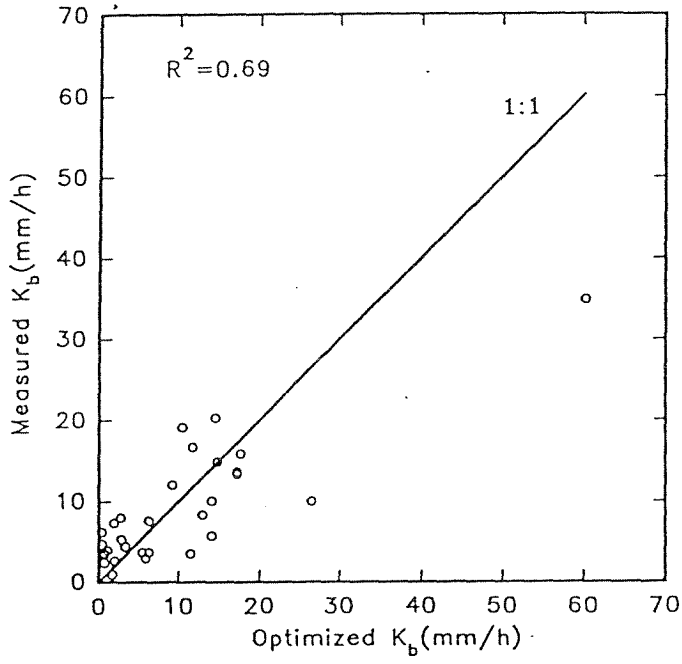

Figure 7.9.2 Baseline hydraulic conductivity values for the time-variable case measured under rainfall simulation compared to those calibrated from curve number predictions.

7.9.2 Cropland Temporally-varying Case: Fallow Soil Adjustments to Effective Conductivity

In the natural system the hydraulic conductivity of the soil matrix is dynamically responding to changes in the surrounding environment. Therefore, to improve the accuracy of infiltration estimates obtained from the Green-Ampt equation in continuous simulation models, reliable estimates of the hydraulic conductivity during each event are necessary. This requires not only an appropriate input value, but also a method for adjusting the hydraulic conductivity to account for temporal changes in the physical condition of the soil. The method which is used to adjust the effective hydraulic conductivity parameter in the WEPP model was based on the results of a study which used over 220 plot years of natural runoff plot data from 11 different locations. By optimizing the effective Green-Ampt hydraulic conductivity for each event within a simulation, a method of determining the temporal variability in the hydraulic conductivity function was established (Risse, 1994). After a detailed statistical analysis of several different WEPP parameters and functions, the following equation was selected to account for the effects of soil crusting and tillage on the effective hydraulic conductivity:

$$K_{bare} = K_b[\, CF + (1 - CF)\, e^{-C\, E_a\, (1 - RR_t/0.04)}\,] \qquad [7.9\text{-}3]$$

where K_{bare} and K_b are the effective conductivity for any given event and the baseline hydraulic conductivity ($mm \cdot h^{-1}$), CF is the crust factor which ranges from 0.20 to 1.0, C is the soil stability factor ($m^2 \cdot J^{-1}$), E_a is the cumulative kinetic energy of the rainfall since the last tillage operation ($J \cdot m^{-2}$), and

RR_i is the random roughness of the soil surface (m). This equation has a similar form to the relationships which have been proposed by Van Doren and Allmaras (1978), Eigel and Moore (1983), and Brakensiek and Rawls (1983). By selecting this form for the equation, it was assumed that the value of K_b will represent a freshly-tilled or maximum hydraulic conductivity which will decrease exponentially at a rate proportional to the kinetic energy of the rainfall since last tillage as it approaches the fully-crusted or final value. While this form is consistent with those in the literature, most of those have been used to calculate the hydraulic conductivity at some time within a given event rather than for a series of successive events. Generally, the energy associated with the rainfall rather than the amount is thought to control the rate at which the surface seal forms. The random roughness term is important, as crusts rarely form on surfaces with random roughness greater than 4 cm and the reduction of effective hydraulic conductivity due to the crust will generally be more significant on smoother surfaces (Rawls et al., 1990).

The crust factor, CF, provides a means of estimating the final or fully-crusted hydraulic conductivity based on the baseline values. The fully-crusted hydraulic conductivity is simply the baseline value multiplied by the crust factor. A relationship developed by Rawls et al. (1990) which states:

$$CF = \frac{SC}{\left[1 + \frac{\Psi}{100\,L}\right]} \qquad [7.9.4]$$

where SC is the correction factor for partial saturation of the subcrust soil, Ψ is the steady state capillary potential at the crust/subcrust interface, and L is the wetted depth (m). They also derive the following continuous relationships for SC and Ψ:

$$SC = 0.736 + 0.19\ sand \qquad [7.9.5]$$

$$\Psi = 45.19 - 46.68\ SC \qquad [7.9.6]$$

The depth to the wetting front is calculated in the WEPP model as:

$$L = 0.147 - 0.15\ (sand)^2 - 0.0003\ (clay)\ \rho_b \qquad [7.9.7]$$

where ρ_b is the bulk density ($kg \cdot m^{-3}$). If the calculated value of L is less than the crust thickness (0.005 m in WEPP) then it is set equal to the crust thickness. Rawls et al. (1990) used data from 36 covered and uncovered plots to validate the fact that this method could provide reasonable estimates of crusted hydraulic conductivities based on freshly-tilled hydraulic conductivities. Table 7.9.3 compares the crust factor calculated using these equations to two values of maximum adjustment taken from the natural runoff plot data.

At six of the ten sites, the calculated crust factor was within 10% of the maximum adjustment calculated from the data. At Bethany and Castana, the reduction in hydraulic conductivity was not as significant as that predicted by the crust factor, while the data from Holly Springs indicated that the crust factor should have been slightly higher. The data indicated that the crust factor calculated by the equations of Rawls et al. (1990) can adequately predict the maximum reduction in conductivity due to crust formation.

Table 7.9.3. Comparison of optimized and calculated values for the crust factors and soil stability constants.

Site	Avg. K_e for events w/ rfcum<1.0	Avg. K_e for 10 events w/ max. rfcum	*CF* calc. from K_f/K_b	*CF* optimum from SAS	*CF* from Rawls et al. (1990)	Optimum *C* $(m^2 \cdot J^{-1})$	Calculated *C* $(m^2 \cdot J^{-1})$
Bethany	1.72	0.61	0.35	0.77	0.20	0.0001	0.0051
Castana	1.87	1.18	0.63	0.63	0.27	0.0002	0.0001
Geneva	4.35	1.85	0.42	0.27	0.37	0.0020	0.0041
Holly Springs	1.40	0.11	0.08	0.27	0.29	0.0009	0.0036
Madison	3.84	0.70	0.18	0.33	0.20	0.0007	0.0001
Morris	11.57	2.11	0.18	0.23	0.27	0.0034	0.0033
Pendleton	*	0.45	*	0.14	0.28	0.0015	0.0026
Presque Isle	4.13	1.18	0.28	0.16	0.38	0.0033	0.0014
Tifton	13.18	2.16	0.20	0.20	0.20	0.0118	0.0122
Watkinsville	8.13	2.73	0.20	0.55	0.20	0.0312	0.0295

* Pendleton did not have any events with less than 80 mm of rainfall since last tillage.

The soil stability factor, *C*, represents the rapidity that the effective conductivity declines from K_b to its fully-crusted value. The values obtained by fitting Eq. [7.9.3] to the optimized effective conductivities for the natural runoff plot data ranged from 0.00006 to 0.0312 $m^2 \cdot J^{-1}$. This generally agreed with the range of values reported in the literature (0.00012-0.0356). For this equation to be widely applicable, the user must have a method for obtaining accurate values of *C* since few measured values are readily available. Regression analysis between the *C* values given in Table 7.9.3 and soil properties indicated that the primary soil factors influencing the rate of surface seal development were sand content (r=0.68), bulk density (r=0.66), and silt content (r=-0.72). Bosch and Onstad (1988) had similar findings in a study they conducted. Based on these findings, the following equation was developed to estimate the soil stability factor based on soil properties:

$$C = -0.0028 + 0.0113\, sand + 0.125 \left[\frac{clay}{CEC}\right] \qquad [7.9.8]$$

where *CEC* is the cation exchange capacity (*meq*/100*g*). Bounds of $0.0001<C<0.010$ were imposed on this equation to prevent negative *C* values on soils with very low sand and clay contents. Using this equation, soils with high amounts of sand or clay and a low CEC will be predicted to form crust more rapidly. Eq. [7.9.8] provided estimates of *C* which were within one order of magnitude of the optimized values for eight of the ten sites (Table 7.9.3).

Figure 7.9.3 shows the optimized event conductivities plotted against those calculated using the tillage adjustment with an optimized baseline hydraulic conductivity for soils with a high, medium, and low value of *C*. In these figures, it is evident that the tillage adjustment using the estimated *C* values is accurately predicting the trend of a reduction in K_e with increasing rainfall kinetic energy since last tillage, however, this adjustment does not account for most of the variability in the K_{opt} values.

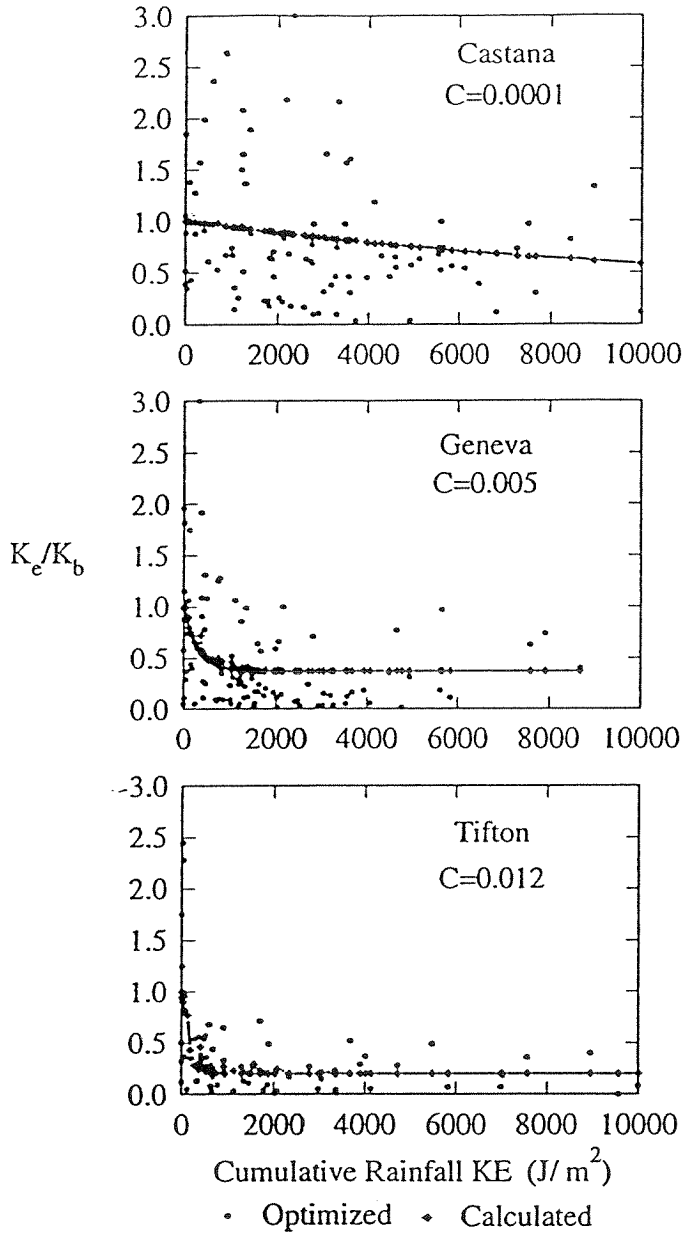

Figure 7.9.3. Comparison of optimized effective conductivities to effective conductivities predicted by the proposed tillage adjustments at three sites.

To compare the effects of using each of these adjustments on predicted runoff amounts, each adjustment was incorporated into WEPP. Two different developmental WEPP versions were tested; 1) a constant K_{ec} version in which no temporal variation was allowed; and 2) a version which included the tillage and crusting adjustments. Both versions were run using calibrated values of hydraulic conductivity. The optimized baseline conductivities and model efficiencies of each of the versions is given in Table 7.9.4.

The baseline values of hydraulic conductivity were all higher than the effective conductivities obtained for the constant value version. This was expected since the constant values represent the

average effective conditions rather than the freshly-tilled conditions. Using the tillage adjustment the average effective value, K_{ec} was approximately 42% of K_b. The average model efficiency was higher for the version of the model which used the tillage adjustment and this version performed the better at nine of the eleven sites. The correlation coefficients, r^2, were generally close to the model efficiencies and indicated the same trends. The slope and intercept of the regression line between measured and predicted values can be used as a measure of bias.

Table 7.9.4. Comparison of optimized baseline conductivities and model results for WEPP using constant values of hydraulic conductivity and temporally varying values.

	Constant K_{ec} ($mm \cdot h^{-1}$)					K_b ($mm \cdot h^{-1}$) with tillage and crusting adjustment				
Site	K_{ec}	ME*	Slp.	Int.	r^2	K_b	ME	Slp	Int	r^2
Bethany	1.22	0.81	0.90	0.02	0.81	3.65	0.82	0.91	0.81	0.82
Castana	2.04	0.46	0.82	0.50	0.59	2.38	0.49	0.84	0.05	0.62
Geneva	2.27	0.63	0.83	0.67	0.67	5.14	0.72	0.80	0.32	0.74
Guthrie	6.19	0.85	0.97	-0.99	0.87	16.73	0.85	0.97	-1.04	0.87
Holly Springs	0.31	0.84	0.87	1.39	0.84	0.72	0.87	0.85	1.82	0.87
Madison	1.80	0.74	0.69	1.57	0.75	2.01	0.77	0.71	1.42	0.78
Morris	7.68	0.40	0.69	0.05	0.52	16.41	0.59	0.74	-0.29	0.66
Pendleton	0.51	0.07	0.61	-0.18	0.41	1.76	0.07	0.67	-0.12	0.41
Presque Isle	2.38	0.19	0.55	1.12	0.36	3.82	0.46	0.63	0.68	0.53
Tifton	7.87	0.49	0.79	0.77	0.59	18.14	0.66	0.85	2.19	0.69
Watkinsville	4.41	0.84	0.97	-0.81	0.86	19.15	0.84	1.01	-1.13	0.87
Average		0.56	0.79	0.37	0.66		0.65	0.82	0.43	0.71

* Model efficiency calculated between WEPP predicted runoff and measured values. Regression statistics calculated between measured and predicted runoff.

The results from a perfect model would have a slope of one and a intercept of zero. For both versions of the model and almost every site, the slopes were less than one and the intercepts were greater than zero. This indicates that both of the versions were over-predicting runoff for the smaller events and under-predicting runoff for the larger events. The version with the tillage adjustment appeared to be less biased as it had a higher slope.

7.9.3 Cropland Temporally-Varying Case: Cropping Adjustments to Effective Conductivity

7.9.3.1 Temporal Adjustment for Row Crops

Surface cover is known to be effective in reducing soil crusting and increasing effective hydraulic conductivity (K_e). Flow through macropores formed by root and soil fauna under cropped conditions plays an important role in increasing K_e. As compared to the corresponding fallow conditions, the degree of the increase under cropped conditions heavily depends on crop and residue management practices, tillage systems, soil properties, and rainfall characteristics, as well as their interactions. Wischmeier (1966) observed that water infiltration was more a characteristic of surface conditions and management than of a specific soil type, and that infiltration increased with larger storms. This indicates that the effects of these variables and their interactions must be considered in order to successfully apply the Green-Ampt equation to cropped conditions.

A total of 328 plot-years of data from natural runoff plots on 8 sites with 1912 measured runoff values were used to develop equations for adjusting K_e for row cropped conditions (Table 7.9.5). The management input files were compiled based on recorded data. Plant growth parameters were calibrated to obtain realistic above-ground biomass. Soil, slope, and climate input files were prepared using measured data. Events which accounted for about 60-70% of the total annual runoff were strictly selected from each site based on data quality.

Table 7.9.5. Site and crop management descriptions.

Site	Crop management	Number of reps	Years	Number of events
Holly Springs,MS	a. fallow	2	1961-68	208
slope: 0.05 m/m	b. cont. corn, sprint TP†	2	1961-68	163
size: 4x22.3 m				
Madison,SD	a. fallow	3	1962-70	59
slope: 0.06 m/m	b. cont. corn, spring TP	3	1962-70	48
size:4x22.3 m	c. cont. corn, no TP	3	1962-70	50
	d. cont. oats	3	1962-64	15
Morris, MN	a. fallow	3	1962-71	67
slope:0.06 m/m	b. cont. corn, fall TP	3	1962-71	67
size:4x22.3 m				
Presque Isle, ME	a. fallow	3	1961-65	65
slope: 0.08 m/m	b. cont. potato	3	1961-65	64
size: 3.7x22.3 m				
Watkinsville, GA	a. fallow	2	1961-67	147
slope: 0.07 m/m	b. cont. corn, spring TP	2	1961-67	97
size: 4x22.3 m	c. cont. cotton, spring TP	2	1961-67	112
Bethany, MO	a. fallow	1	1931-40	109
slope: 0.07 m/m	b. cont. corn, spring TP	1	1931-40	112
size: 4.3x22.3 m				
Geneva, NY	a. fallow	1	1937-46	97
slope: 0.08 m/m	b. summer fallow, winter rye	1	1937-46	77
size: 1.8x22.3 m	c. cont. soybean, spring TP	1	1937-46	45
Guthrie, OK	a. fallow	1	1942-56	170
slope: 0.08 m/m	b. cont. cotton, spring TP	1	1942-56	140
size: 1.8x22.3 m				

† TP, turn plow

Canopy height has a significant effect on surface runoff (Khan et al., 1988). Based on the measured fall velocities for a raindrop size (diameter) of 2.5 mm at various fall heights (Laws, 1941), the following correction factor (C_h) for canopy height effectiveness as cover relative to infiltration was developed

$$C_h = e^{\left[-0.33\,\frac{h}{2}\right]} \qquad r^2 = 0.99 \qquad [7.9.9]$$

where h is the fall height in meters. Average fall height was calculated as one half of the crop height in WEPP. With Eq. [7.9.9], the effective canopy cover (*ccovef*) can be computed by

$$ccovef = cancov\ C_h \qquad [7.9.10]$$

where *cancov* is the canopy cover (0-1).

The total effective surface cover (*scovef*) can be computed by

$$scovef = ccovef + rescov - (ccovef)\,(rescov) \qquad [7.9.11]$$

where *rescov* is the residue cover (0-1).

Correlation coefficients of selected variables to optimized K_e for each site are tabulated in Table 7.9.6. For cover-related variables, the correlation coefficients from the pooled data increased in the order of: *cancov*, *ccovef*, *rescov*, and *scovef*. This sequence implies that 1). The adjustment of canopy cover by Eq. [7.9.10] is useful; 2). Residue cover is more correlated to K_e than canopy cover; 3). The combined effects of the two are greater than either one of them when used alone. The rainfall amount (*rain*) showed a very strong correlation with K_e. This behavior could be explained by macropore flow phenomena. More importantly, the product of *rain* and *scovef* exhibited a better overall correlation coefficient than either *rain* or *scovef*, indicating a positive interaction between the two. Thus, this interactive product should be a better predictor for K_e.

Table 7.9.6. Correlation coefficients of selected variables to optimized event hydraulic conductivities.

Site	Canopy cover (*cancov*)	Effective canopy cover (*ccovef*)	Residue cover (*rescov*)	Total effective surface cover (*scovef*)	Residue mass on ground	Buried residue mass	Total root mass	Days since last tillage	Rainfall amount (*rain*)	Rainfall &cover term†
Holly Springs	.11	.11	.26	.27	.24	.17	.31	.20	.31	.41
Madison	.20	.19	.03‡	.17	.07‡	.08‡	.17	-.01‡	.28	.32
Morris	.04‡	.05‡	-.02‡	.05‡	-.01‡	-.04‡	.04‡	-.15‡	.68	.20
Presque Isle	-.04‡	-.04‡	-.16‡	-.08‡	.00‡	.04‡	.01‡	-.05‡	.33	.06
Watkinsville	.18	.19	.20	.31	.18	.28	.31	.05‡	.40	.49
Bethany	.16	.17	-.10‡	.14	-.09‡	.12‡	.06‡	.00‡	.27	.22
Geneva	.43	.42	.27	.49	.28	.37	.49	.08‡	.64	.82
Guthrie	.14	.15	.06‡	.16	.05‡	.30	.27	-.18	.42	.28
pooled*	.10	.12	.13	.20	.14	.17	.06	.11	.38	.39

† Rain*scovef

‡ Not significant at 5% level.

* Using the lumped database from all the sites.

Based on the above analyses, the final model structure was proposed as:

$$K_e = K_{bare}\,(1 - scovef) + (c\ rain\ scovef) \qquad [7.9.12]$$

where K_{bare} is the K_e of the bare area ($mm \cdot h^{-1}$) and can be estimated by Eq. [7.9.3], c is a regression coefficient and was estimated for each soil series at each site, and *rain* is the storm rainfall amount in millimeters. This equation assumes that K_e for any given area can be conceptualized as the areally-weighted average of K_{bare} and K_e in the covered area. The latter, being closely related to the variable of *rain*scovef*, can be well represented by this variable. This model formulation attempts to reflect the general conditions. For the fallow case, Eq. [7.9.12] reduces to $K_e = K_{bare}$. While under the fully-covered conditions, the effect of soil crusting is neglected and K_e is adjusted for the effects of surface cover and rainfall amount. The c values were strongly related to basic soil properties such as sand and clay content, and to K_b which is estimated from basic soil properties (Eqs. [7.9.1] and [7.9.2]). The relationship to K_b can be described by :

$$c = 0.0534 + 0.01179\,(K_b) \qquad [7.9.13]$$

where K_b is in $mm \cdot h^{-1}$. Substituting the above equation for c, the final adjustment equation becomes:

$$K_e = K_{bare}\,(1 - scovef) + (0.0534 + 0.01179\,K_b)\,(rain)\,(scovef) \qquad [7.9.14]$$

The predicted mean K_e and total WEPP predicted runoff using Eq. [7.9.14], along with measured values, are presented in Table 7.9.7. The predicted mean K_e agreed well with the optimized mean K_e. The total measured runoff of the selected events and the total predicted runoff matched well with r^2 and slope of regression being 0.94 and 0.99, respectively. The model efficiency, calculated on an event basis, averaged 0.64, which indicates that Eq. [7.9.14] works better than just using a constant mean for K_e.

This can also be clearly seen in Fig. 7.9.4. In addition, the seasonal variation of K_e and runoff were also represented by the equation.

Table 7.9.7. Total rainfall, optimized and predicted effective conductivity (K_e), and measured and predicted total runoff for the selected events.

Site	Management	Total rainfall	K_e†		Total runoff		Model efficiency‡ (*ME*)
			Optimized	Predicted	Measured	Predicted	
		mm	------- $mm \cdot h^{-1}$ -------		------- *mm* -------		
Holly Springs	fallow	5742	0.53				
	corn	5049	1.34	1.20	1793	2014	.582
Madison	fallow	1553	1.54				
	corn TP	1310	1.83	1.62	322	311	.783
	corn No TP	1359	1.76	1.75	311	275	.747
	oats	410	1.86	1.76	86	88	.775
Morris	fallow	1985	5.85				
	corn	1987	6.11	6.74	319	310	.340
Presque Isle	fallow	1321	1.53				
	potato	1296	1.57	2.75	432	231	.291
Watkinsville	fallow	4277	3.34				
	corn	3566	8.45	9.66	675	793	.823
	cotton	3846	7.36	8.65	834	911	.791
Bethany	fallow	3330	1.42				
	corn	3375	1.73	1.60	1375	1308	.845
Geneva	fallow	2292	2.40				
	winter rye	1912	3.95	2.91	375	534	.511
	soybean	1446	8.70	3.66	51	338	**
Guthrie	fallow	5313	5.58				
	cotton	4820	8.16	8.87	1239	1204	.793

† Means of all selected events calculated on an event basis.

‡ Calculation on an event basis.

** Indicates negative model efficiency.

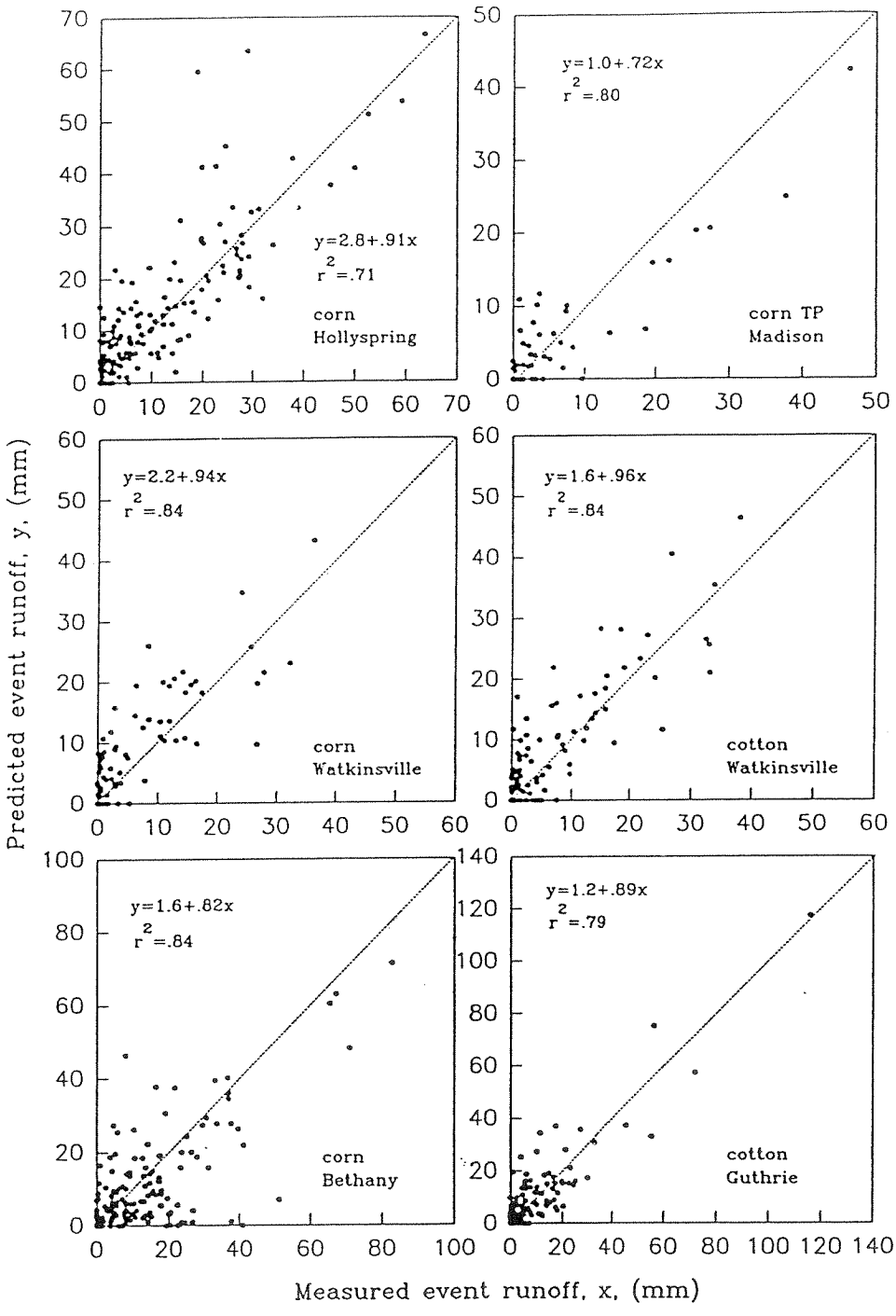

Figure 7.9.4. Measured vs. predicted runoff for each individual storm on selected sites under row crop conditions.

7.9.3.2 Temporal Adjustment for Perennial Crops

The sites used for row crop adjustment were also used for perennial crops except for the Madison site where perennial crops were not grown (Table 7.9.8). Therefore, the same climate, slope, and soil input files were used. The management input files were prepared according to the recorded data, and the plant growth parameters were calibrated. Two common cropping systems, continuous meadow and rotation meadow, were included. A total of 88 plot-years of data with 506 measured runoff values were used for the validation.

Table 7.9.8. Background information of the database used for K_e adjustment under perennial crops.

Site	Crop Management	Number of reps	Periods used	Years in meadow	Number of events used
Holly Springs, MS	meadow-corn-meadow	2	1962-68	5	101
Morris, MN	meadow-corn-oats	3	1962-71	4	18
Presque Isle, ME	potato-oats-meadow	3	1961-65	1	4
Watkinsville, GA	corn-meadow-meadow	2	1961-67	4	44
Bethany, MO	cont. alfalfa	1	1931-40	10	83
	cont. blue grass	1	1931-40	10	79
Geneva, NY	cont. red clover	1	1937-41	5	19
	cont. blue grass	1	1937-46	10	30
Guthrie, OK	cont. blue grass	1	1942-56	15	96
	wheat-meadow-cotton	1	1942-56	5	32

Since similar correlation relationships between the selected variables and optimized K_e values existed for both row crops and perennial crops, Eq. [7.9.2] was used to generate the first approximation of effective hydraulic conductivity (K_{appr}) for each event under meadow conditions. The mean optimized K_e and mean generated K_{appr} on the 7 sites were used to develop the following adjustment equation

$$K_e = 1.81\ (K_{appr}) \qquad [7.9.15]$$

where K_{appr} is in $mm \cdot h^{-1}$ and can be replaced by Eq. [7.9.14].

$$K_e = 1.81\ (K_{bare}\ (1 - scovef) + (0.0534 + 0.01179\ K_b)\ (rain)\ (scovef) \qquad [7.9.16]$$

This final adjustment equation shows that with identical effective surface cover (scovef) the K_e of perennial crops is approximately 1.8 times higher than that from the corresponding row cropped conditions. This is due to the fact that perennial crops, often accompanied by the formation of a thick layer of organic matter or plant residue on soil surface, are more effective in improving soil aggregation, controlling soil crusting, and forming and preserving bio-pores.

As is shown in Table 7.9.9, the optimized K_e and predicted K_e matched well. The coefficient of determination for predicted mean K_e versus the optimized values was 0.90 and slope of regression was 0.96. The total runoff from the selected events was also predicted well. The r^2 and slope of regression were 0.94 and 0.99, respectively. Model efficiency, calculated on an event basis, averaged 0.49 (Table

7.9.9), indicating the individual storm runoff was predicted reasonably well. The predicted and measured annual runoff was plotted in Fig. 7.9.5. Linear regression fit the data well (r^2=0.76) with little bias (slope=0.88).

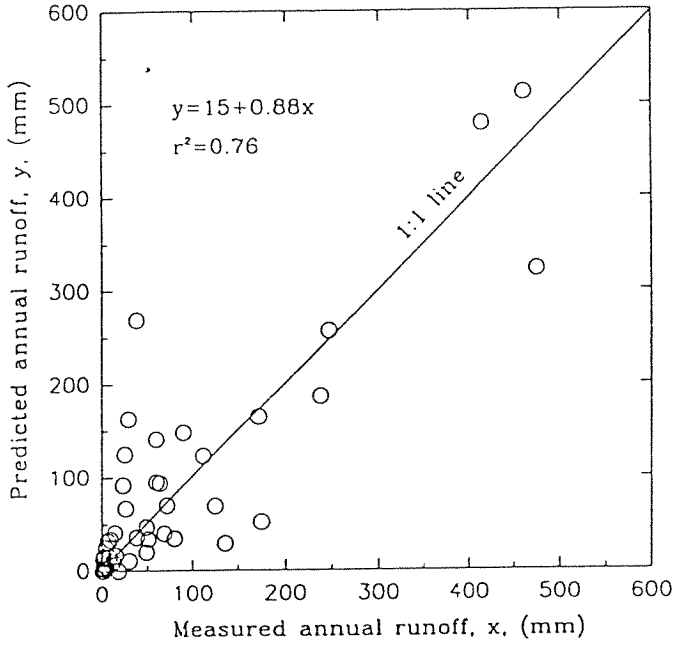

Figure 7.9.5. Measured vs. predicted annual runoff for the data used under meadow conditions.

Table 7.9.9. Total rainfall, optimized and predicted effective conductivity (K_e), and measured and predicted total runoff for the events selected in the years when meadow was grown.

Site	Crop Management	Total Rainfall (*mm*)	K_e† Optimized ($mm \cdot h^{-1}$)	K_e† Predicted ($mm \cdot h^{-1}$)	Total runoff Measured (*mm*)	Total runoff Predicted (*mm*)	Model Efficiency (*ME*)‡
Holly Springs	bermuda-corn-bermuda	3497	1.62	2.49	1196	1256	.675
Morris	grass-corn-oats	646	12.15	17.55	27	17	.649
Watkinsville	corn-bermuda-bermuda	1682	11.87	13.36	154	269	.573
Bethany	cont. alfalfa	2900	6.40	4.98	310	553	.290
	cont. brome grass	2761	5.47	5.90	308	265	.466
Geneva	cont. red clover	549	6.71	6.54	35	54	--
	cont. brome grass	1131	10.23	7.97	3	93	--
Guthrie	cont bermuda grass	3767	19.55	20.30	189	373	.734
	wheat-clover-cotton	1270	13.81	22.19	112	145	.275

† Means of all selected events.

‡ Calculated on an event basis, and negative *ME* is not presented.

7.9.4 Cropland Time-Invariant Effective Hydraulic Conductivity Values

For the case of time-invariant effective conductivity, the input value of K_e must represent both the soil type and the management practice. This method is corollary to the curve number approach for predicting runoff, and in fact, the estimation procedures discussed here were derived using curve number optimizations, so the runoff volumes predicted should correspond closely to curve number predictions. One difference between this method and the curve number method is that no soil moisture correction is necessary, since WEPP takes into account moisture differences via internal adjustments to the wetting front matric potential term of the Green-Ampt equation.

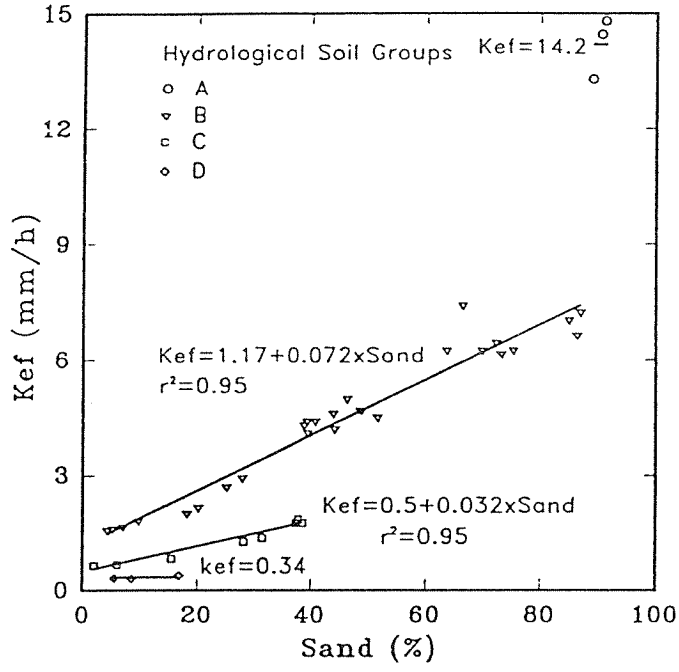

Figure 7.9.6. Optimized effective conductivity values for fallow soil conditions, K_{ef}, plotted versus sand content of the soil. This is for the case of time-invariant conductivity.

The estimation procedure involves two steps. In step one a fallow soil K_{ef} is calculated. In step 2 the fallow soil K_{ef} is adjusted based on management practice using a runoff ratio to obtain the input value of K_{ec}.

Step 1: K_{ef} was found to be related to the amount of sand in the upper 20 cm of the soil profile (Fig. 7.9.6). Thus, one may use the hydrologic soil group and sand content to estimate K_{ef} ($mm \cdot h^{-1}$):

Hydrologic Soil Group	Formula
A	$K_{ef} = 14.2$
B	$K_{ef} = 1.17 + 7.2(sand)$
C	$K_{ef} = 0.50 + 3.2(sand)$
D	$K_{ef} = 0.34$

Step 2: Multiply K_{ef} by the value in the table below to obtain K_e ($mm \cdot h^{-1}$):

	Hydrologic Soil Group		
	A	B,C	D
Fallow	1.00	1.00	1.00
Conv. Tillage - Corn	1.35	1.58	1.73
Conv. Tillage - Soybeans	1.39	1.70	2.00
Conserv. Till. - Corn	1.48	1.79	2.21
Conserv. Till. - Soybeans	1.50	1.91	2.49
Small Grain	1.84	2.14	2.48
Alfalfa	2.86	3.75	6.23
Pasture (Grazed)	3.66	4.34	5.96
Meadow (Grass)	6.33	9.03	15.5

For other cases, such as for crop rotations, ratios of K_e/K_{ef} may be estimated from curve number values using the equation:

$$K_{ec} = \frac{56.82\ K_{ef}^{0.286}}{1 + 0.051e^{0.062CN}} - 2 \qquad [7.9.17]$$

Table 7.9.10 shows the model results as applied to data from fallow natural runoff plots. The tests indicate that this method gives a slightly better fit to the measured data than does the curve number method, as evidenced by the greater event-by-event model efficiencies. Tables 7.9.11 and 7.9.12 show the model results as applied to data from several cropped natural runoff plots. In Table 7.9.11, Eq. [7.9.17] was used to estimate K_{ec}, whereas the ratio values listed above for the 7 management practices were used in Table 7.9.12. WEPP produced better model efficiencies for most of the applications than did the curve number procedure.

Table 7.9.10. Measured runoff volumes, curve numbers and WEPP predicted runoff volumes, and model efficiency for the fallow runoff plot data.

Site	Average runoff per event (*mm*)			Model efficiency	
	Measured	CN	WEPP	CN	WEPP
Bethany, MO	14.43	10.03	10.72	0.72	0.77
Castana, IA	11.47	11.87	14.41	0.10	0.11
Geneva, NY	7.87	6.08	6.45	0.58	0.63
Guthrie, OK	10.91	10.58	12.46	0.77	0.80
Holly Springs, MS	15.17	12.62	13.58	0.79	0.84
Madison, SD	7.96	6.72	9.40	0.69	0.70
Morris, MN	5.55	8.77	10.94	-1.06	-1.20
Pendleton, OR	3.18	1.87	1.24	-0.26	-0.08
Presque Isle, ME	6.91	4.87	4.86	-0.25	0.18
Tifton, GA	19.58	21.70	21.17	0.36	0.43
Watkinsville, GA	13.42	11.98	13.41	0.75	0.83

Table 7.9.11. Measured runoff volumes, curve number and WEPP predicted runoff volumes, and model efficiency for the cropped runoff plot data. The estimations of effective conductivity are from the use of Eq. [7.9.17].

Site	Management Practice	Average runoff per event (*mm*)			Model efficiency	
		Measured	Curve Number	WEPP	Curve Number	WEPP
Bethany, MO	Alfalfa	3.72	1.25	1.41	0.33	0.49
Bethany, MO	Blue grass	3.91	1.30	1.28	0.43	0.42
Bethany, MO	Corn	12.20	6.65	7.63	0.66	0.73
Guthrie, OK	Blue grass	1.94	2.04	4.88	0.58	0.32
Guthrie, OK	Cotton	8.85	9.03	14.21	0.68	0.49
Holly Springs, MS	Corn	11.00	11.91	12.01	0.15	0.38
Madison, SD	Corn	6.70	4.90	6.07	0.55	0.78
Madison, SD	No-till corn	6.22	3.57	4.75	0.50	0.76
Watkinsville, GA	Corn	6.96	9.97	14.15	0.37	0.04
Watkinsville, GA	Cotton	7.48	8.91	12.22	0.49	0.09

Table 7.9.12. Measured runoff volumes, curve number and WEPP predicted runoff volumes, and model efficiency for the cropped runoff plot data. The estimations of effective conductivity are from the use of tabulated values in the text.

Site	Management Practice	Average runoff per event (*mm*)			Model efficiency	
		Measured	Curve Number	WEPP	Curve Number	WEPP
Bethany, MO	Alfalfa	3.72	1.25	1.46	0.33	0.50
Bethany, MO	Blue grass	3.91	1.30	1.33	0.43	0.43
Bethany, MO	Corn	12.20	6.65	7.55	0.66	0.72
Guthrie, OK	Blue grass	1.94	2.04	2.74	0.58	0.80
Guthrie, OK	Cotton	8.85	9.03	11.46	0.68	0.68
Holly Springs, MS	Corn	11.00	11.91	13.35	0.15	0.29
Madison, SD	Corn	6.70	4.90	7.56	0.55	0.70
Madison, SD	No-till corn	6.22	3.57	5.91	0.50	0.76
Watkinsville, GA	Corn	6.96	9.97	11.44	0.37	0.37
Watkinsville, GA	Cotton	7.48	8.91	10.50	0.49	0.55

7.9.5 Cropland Bio-pore Adjustments to Effective Conductivity

Accounting for infiltration differences as a function of wormholes may be made by adjusting the input value of effective conductivity. The suggestions listed here are preliminary guidelines which are based on interpretations of personal communications regarding the effects of bio-pores on permeability classes from the SCS Soil Survey Laboratory Staff. The first step is to identify the bio-pore influence class from Table 7.9.13 below. Then, the input value of either K_{ec} or K_b as calculated above should be multiplied by the ratio shown in Table 7.9.14 below.

Table 7.9.13. Classes of bio-pore influence defined by abundance and size classes.

	Pore Size		
Abundance	Medium	Coarse	Very Coarse
Few	Small	Moderate	Moderately Large
Common	Moderate	Moderately Large	Large
Many	Moderately Large	Large	Very Large

Table 7.9.14. Increase in input K_{ec} or K_b by bio-pore influence.

Input K_{ec},K_b	Bio-pore Influence	Ratio for K_{ec}, K_b Increase
Very Low	Moderate	12
<0.5 $mm \cdot h^{-1}$	Large	15
	Very Large	18
Low	Moderate	9
0.5-1 $mm \cdot h^{-1}$	Large	12
	Very Large	15
Moderately Low	Moderate	6
1-2 $mm \cdot h^{-1}$	Large	9
	Very Large	12
Moderate	Moderate	3
2-3 $mm \cdot h^{-1}$	Large	6
	Very Large	9
Moderately High	Moderate	2
3-5 $mm \cdot h^{-1}$	Large	2.5
	Very Large	3

7.9.6 Rangeland Effective Hydraulic Conductivity Estimation

Baseline default equations for predicting K_e on rangelands were developed from rainfall simulation data collected on 150 plots from 34 locations across the western United States. The data were collected during the WEPP rangeland field experiment and as a part of a joint Agricultural Research Service and Natural Resource Conservation Service project known as the Interagency Rangeland Water Erosion Team (IRWET). Site description information for each location is given in Tables 7.9.15 and 7.9.16. K_{erange} for each of the 150 plots was obtained by optimizing the WEPP model based on total runoff volume (mm). Multiple regression procedures were then used to develop predictive equations for K_{erange} based on both biotic and abiotic plot-specific properties. The resulting equations are as follows.

If the rill surface cover (surface cover outside the plant canopy) is less than 45%, then K_{erange} is predicted from:

$$K_{erange} = 57.99 - 14.05\, ln\,(CEC) + 6.20\, ln\,(ROOT10) - 473.39\, BASR^2 + 4.78\, RESI \qquad [7.9.18]$$

where CEC is cation exchange capacity of the surface soil ($meq/100g$), $ROOT10$ is root biomass in the top 10 cm of the soil ($kg \cdot m^{-2}$), $BASR$ is the fraction of basal surface cover in rill (outside the plant canopy) areas based on the entire overland flow element area (0-1), and $RESI$ is the fraction of litter surface cover in interrill (under plant canopy) areas based on the entire overland flow element area (0-1). $BASR$ is the product of the fraction of basal surface cover in rill areas ($FBASR$, expressed as a fraction of total basal surface cover) and total basal surface cover ($BASCOV$). $RESI$ is the product of the fraction of litter surface cover in interrill areas ($FRESI$, expressed as a fraction of total litter surface cover) and total litter surface cover ($rescov$).

If rill surface cover is greater than or equal to 45%, then K_{erange} is predicted from:

$$K_{erange} = -14.29 - 3.40\, ln\,(ROOT10) + 37.83\, sand + 208.86\, orgmat + 398.64\, RR - 27.39\, RESI + 64.14\, BASI \qquad [7.9.19]$$

where $sand$ is the fraction of sand in the soil (0-1), $orgmat$ is the fraction of organic matter in the soil (0-1), RR is the soil surface random roughness (m), and $BASI$ is the fraction of basal surface cover in interrill areas based on the entire overland flow element area (0-1). $BASI$ is the product of the fraction of basal surface cover in interrill areas ($FBASI$, expressed as a fraction of total basal surface cover) and total basal surface cover ($BASCOV$).

The user is cautioned against using Eqs. [7.9.18] and [7.9.19] with data which fall outside the ranges of data values upon which the regression equations were developed. Ranges of values for each variable used in the equation development are given in Table 7.9.17.

Table 7.9.15. Abiotic mean site characteristics and optimized effective hydraulic conductivity ($mm \cdot h^{-1}$) values from WEPP Rangeland and USDA-IRWET[1] rangeland rainfall simulation experiments used to develop the baseline effective hydraulic conductivity equation for the WEPP model.

Location	Soil family	Soil series	Surface texture	Slope (%)	Organic matter (%)	Bulk density[2] ($g \cdot cm^{-3}$)	Mean optimized K_e	Range in optimized K_e min.	max.
1) Prescott, AZ	Aridic argiustoll	Lonti	Sandy loam	5	1.3	1.6	7.0	4.1	9.8
2) Prescott, AZ	Aridic argiustoll	Lonti	Sandy loam	4	1.3	1.6	5.6	3.4	6.9
3) Tombstone, AZ	Ustochreptic calciorthid	Stronghold	Sandy loam	10	1.8	1.5	28.7	24.5	32.9
4) Tombstone, AZ	Ustollic haplargid	Forrest	Sandy clay loam	4	1.5	1.5	8.7	3.6	13.8
5) Susanville, CA	Typic argixeroll	Jauriga	Sandy loam	13	6.4	1.2	16.7	15.3	18.7
6) Susanville, CA	Typic argixeroll	Jauriga	Sandy loam	13	6.4	1.2	17.2	13.9	20.3
7) Akron, CO	Ustollic haplargid	Stoneham	Loam	7	2.5	1.5	7.3	1.5	15.0
8) Akron, CO	Ustollic haplargid	Stoneham	Sandy loam	8	2.4	1.5	16.5	8.4	23.0
9) Akron, CO	Ustollic haplargid	Stoneham	Loam	7	2.2	1.5	8.8	4.8	14.0
10) Meeker, CO	Typic camborthid	Degater	Silty clay	10	2.4	1.5	8.0	5.2	10.8
11) Blackfoot, ID	Pachic cryoborall	Robin	Silt loam	7	7.5	1.3	7.0	4.7	9.7
12) Blackfoot, ID	Pachic cryoborall	Robin	Silt loam	9	9.9	1.2	7.8	6.6	9.7
13) Eureka, KS	Vertic argiudoll	Martin	Silty clay loam	3	6.0	1.4	2.9	1.1	4.6
14) Sidney, MT	Typic argiboroll	Vida	Loam	10	5.2	1.2	22.5	18.4	26.5
15) Wahoo, NE	Typic argiudoll	Burchard	Loam	10	5.1	1.3	3.3	2.0	4.4
16) Wahoo, NE	Typic argiudoll	Burchard	Loam	11	4.8	1.3	15.3	13.1	17.5
17) Cuba, NM	Ustollic camborthid	Querencia	Sandy loam	7	1.5	1.5	16.5	14.5	18.5
18) Los Alamos, NM	Aridic haplustalf	Hackroy	Sandy loam	7	1.4	1.5	6.3	5.2	7.3
19) Killdeer, ND	Pachic haploborall	Parshall	Sandy loam	11	3.6	1.3	23.2	21.2	25.4
20) Killdeer, ND	Pachic haploborall	Parshall	Sandy loam	11	3.5	1.3	22.4	17.9	26.9
21) Chickasha, OK	Udic argiustoll	Grant	Loam	5	4.0	1.3	17.8	9.4	27.7
22) Chickasha, OK	Udic argiustoll	Grant	Sandy loam[3]	5	2.3	1.5	13.6	8.8	18.8
23) Freedom, OK	Typic ustochrept	Woodward	Loam	6	3.1	1.4	14.9	13.0	16.8
24) Woodward, OK	Typic ustochrept	Quinlan	Loam	6	2.3	1.5	20.4	15.5	25.9
25) Cottonwood, SD	Typic torrert	Pierre	Clay	8	3.2	1.5	9.3	8.6	10.0
26) Cottonwood, SD	Typic torrert	Pierre	Clay	12	3.7	1.4	3.6	2.7	4.4
27) Amarillo, TX	Aridic paleustoll	Olton	Loam	3	3.0	1.5	8.4	6.5	9.7
28) Amarillo, TX	Aridic paleustoll	Olton	Loam	2	2.5	1.5	5.8	2.4	10.4
29) Sonora, TX	Thermic calciustoll	Purbes	Cobbly clay	8	8.9	1.2	2.2	0.8	3.7
30) Buffalo, WY	Ustollic haplargid	Forkwood	Silt loam	10	2.8	1.5	5.9	4.2	8.8
31) Buffalo, WY	Ustollic haplargid	Forkwood	Loam	7	2.4	1.5	4.6	1.7	11.5
32) Newcastle, WY	Ustic torriothent	Kishona	Sandy loam	7	1.7	1.5	21.7	14.8	26.3
33) Newcastle, WY	Ustic torriothent	Kishona	Loam	8	2.2	1.5	23.1	20.0	28.6
34) Newcastle, WY	Ustic torriothent	Kishona	Sandy loam	9	1.4	1.5	9.0	6.3	12.4

[1] Interagency Rangeland Water Erosion Team is comprised of ARS staff from the Southwest and Northwest Watershed Research Centers in Tucson, AZ and Boise, ID, and NRCS staff members in Lincoln, NE and Boise, ID.

[2] Bulk density calculated by the WEPP model based on measured soil properties including percent sand, clay, organic matter and cation exchange capacity.

[3] Farm land abandoned during the 1930's that had returned to rangeland. The majority of the 'A' horizon had been previously eroded.

Table 7.9.16. Biotic mean site characteristics from WEPP Rangeland and USDA-IRWET[1] rangeland rainfall simulation experiments used to develop the baseline effective hydraulic conductivity equations for the WEPP model.

Location	MLRA[2]	Rangeland cover type[3]	Range site	Dominant species by weight descending order	Eco-logical status[4]	Canopy cover (%)	Ground cover (%)	Standing biomass ($kg \cdot ha^{-1}$)
1) Prescott, AZ	35	Grama-Galleta	Loamy upland	Blue grama Goldenweed Ring muhly	54	48	47	990
2) Prescott, AZ	35	Grama-Galleta	Loamy upland	Rubber rabbitbrush Blue grama Threeawn	36	51	50	2,321
3) Tombstone, AZ	41	Creosotebush-Tarbush	Limy upland	Tarbush Creosobush	38	32	82	775
4) Tombstone, AZ	41	Grama-Tobosa-Shrub	Loamy upland	Blue grama Tobosa Burro-weed	55	18	40	752
5) Susanville, CA	21	Basin Big Brush	Loamy	Idaho fescue Squirreltail Wooly mulesears Green rabbitbrush Wyoming big sagebrush	55	29	84	5,743
6) Susanville, CA	21	Basin Big Brush	Loamy	Idaho fescue Squirreltail Wooly mulesears Green rabbitbrush Wyoming big sagebrush	55	18	76	5,743
7) Akron, CO	67	Wheatgrass-Grama-Needlegrass	Loamy plains #2	Blue grama Western wheatgrass Buffalograss	76	54	96	1,262
8) Akron, CO	67	Wheatgrass-Grama-Needlegrass	Loamy plains #2	Blue grama Sun sedge Bottlebrush squirreltail	44	44	86	936
9) Akron, CO	67	Wheatgrass-Grama-Needlegrass	Loamy plains #2	Buffalograss Blue grama Prickly pear cactus	45	28	82	477
10) Meeker, CO	34	Wyoming big sagebrush	Clayey slopes	Salina wildrye Wyoming big sagebrush Western wheatgrass	60	11	42	1,583
11) Blackfoot, ID	13	Mountain big sagebrush	Loamy	Mountain big sagebrush Letterman needlegrass Sandberg bluegrass	15	71	90	1,587
12) Blackfoot, ID	13	Mountain big sagebrush	Loamy	Letterman needlegrass Sandberg bluegrass Prairie junegrass	22	87	92	1,595
13) Eureka, KS	76	Bluestem prairie	Loamy upland	Buffalograss Sideoats grama Little bluestem	45	38	58	526
14) Sidney, MO	54	Wheatgrass-Grama-Needlegrass	Silty	Dense clubmoss Western wheatgrass Needle & thread grass Blue grama	58	12	81	2,141
15) Wahoo, NE	106	Bluestem prairie	Silty	Kentucky bluegrass Dandelion Alsike clover	11	27	80	1,239

Table 7.9.16. (continued)

Location	MLRA[2]	Rangeland cover type[3]	Range site	Dominant species by weight descending order	Ecological status[4]	Canopy cover (%)	Ground cover (%)	Standing biomass ($kg \cdot ha^{-1}$)
16) Wahoo, NE	106	Bluestem prairie	Silty	Primrose Porcupinegrass Big bluestem	37	22	87	3,856
17) Cuba, NM	36	Blue grama-Galleta	Loamy	Galleta Blue grama Broom snakeweed	47	13	62	817
18) Los Alamos, NM	36	Juniper-Pinyon Woodland	Woodland community	Colorado rubberweed Sagebrush Broom snakeweed	NA[5]	16	72	1,382
19) Killdeer, ND	54	Wheatgrass-Needlegrass	Sandy	Clubmoss Sedge Crocus	43	69	96	1,613
20) Killdeer, ND	54	Wheatgrass-Needlegrass	Sandy	Sedge Blue grama Clubmoss	52	71	88	1,422
21) Chickasha, OK	80A	Bluestem prairie	Loamy prairie	Indiangrass Little bluestem Sideoats grama	60	46	94	2,010
22) Chickasha, OK	80A	Bluestem prairie	Eroded prairie	Oldfield threeawn Sand paspalum Scribners dichanthelium Little bluestem	40	14	70	396
23) Freedom, OK	78	Bluestem prairie	Loamy prairie	Hairy grama Silver bluestem Perennial forbs Sideoats grama	30	39	72	1,223
24) Woodward, OK	78	Bluestem-Grama	Shallow prairie	Sideoats grama Hairy grama Western ragweed Hairy goldaster	28	45	62	1,505
25) Cottonwood, SD	63A	Wheatgrass-Needlegrass	Clayey west central	Green needle grass Scarlet globemallow Western wheatgrass	100	46	68	2,049
26) Cottonwood, SD	63A	Blue grama-Buffalograss	Clayey west central	Blue grama Buffalograss	30	34	81	529
27) Amarillo, TX	77	Blue grama-Buffalograss	Clay loam	Blue grama Buffalograss Prickly pear cactus	72	23	97	2,477
28) Amarillo, TX	77	Blue grama-Buffalograss	Clay loam	Blue grama Buffalograss Prickly pear cactus	62	10	87	816
29) Sonora, TX	81	Juniper-Oak	Shallow	Buffalograss Curly mesquite Prairie cone flower Hairy tridens	35	39	68	2,461
30) Buffalo, WY	58B	Wyoming big sagebrush	Loamy	Wyoming big sagebrush Prairie junegrass Western wheatgrass	33	53	59	7,591
31) Buffalo, WY	58B	Wyoming big sagebrush	Loamy	Western wheatgrass Bluebunch wheatgrass Green needlegrass	40	68	60	2,901

Table 7.9.16. (continued)

Location	MLRA[2]	Rangeland cover type[3]	Range site	Dominant species by weight descending order	Ecological status[4]	Canopy cover (%)	Ground cover (%)	Standing biomass ($kg \cdot ha^{-1}$)
32) Newcastle, WY	60A	Wheatgrass-Needlegrass	Loamy plains	Prickly pear cactus Needle-and-thread Threadleaf sedge	21	11	77	1,257
33) Newcastle, WY	60A	Wheatgrass-Needlegrass	Loamy plains	Cheatgrass Needle-and-thread Blue grama	22	56	81	2,193
34) Newcastle, WY	60A	Wheatgrass-Needlegrass	Loamy plains	Needle-and-thread Threadleaf sedge Blue grama	50	32	47	893

[1] Interagency Rangeland Water Erosion Team is comprised of ARS staff from the Southwest and Northwest Watershed Research Centers in Tucson, AZ and Boise, ID, and NRCS staff members in Lincoln, NE and Boise, ID.

[2] USDA - Soil Conservation Service. 1981. Land resource regions and major land resource areas of the United States. Agricultural Handbook 296. USDA - SCS, Washington, D.C.

[3] Definition of Cover Types from: T.N. Shiflet, 1994. Rangeland cover types of the United States, Society for Range Management, Denver, CO.

[4] Ecological status is a similarity index that expresses the degree to which the composition of the present plant community is a reflection of the historic climax plant community. This similarity index may be used with other site criterion or characteristics to determine rangeland health. Four classes are used to express the percentage of the historic climax plant community on the site (I 76-100; II 51-75; III 26-50; IV 0-25). USDA, National Resources Conservation Service. 1995. National Handbook for Grazingland Ecology and Management. National Headquarters, Washington, D.C. in press.

[5] NA - Ecological status indices are not appropriate for woodland communities.

Table 7.9.17. Ranges of values for variables used to develop Eqs. [7.9.18] and [7.9.19].

Variable	Mean	Minimum	Maximum
Equation 7.9.18			
CEC	20	7	45
*ROOT*10	0.45	0.09	0.99
BASR	0.06	0.00	0.27
RESI	0.34	0.05	0.84
Equation 7.9.19			
*ROOT*10	0.69	0.12	1.95
SAND	0.43	0.02	0.71
ORGMAT	0.04	0.02	0.10
RROUGH	0.013	0.005	0.045
RESI	0.16	0.02	0.41
BASI	0.05	0.00	0.34

Eqs. [7.9.18] and [7.9.19] have not been independently validated, however, they have performed well at predicting K_{erange} compared to the data set from which the equations were derived (Figure 7.9.7). The residuals shown in Figure 7.9.8 showed no bias and were similarly distributed between the two equations. Predicted values of K_{erange} were used in the model to predict runoff volume and peak runoff rate and the results are shown in Figures 7.9.9 and 7.9.10.

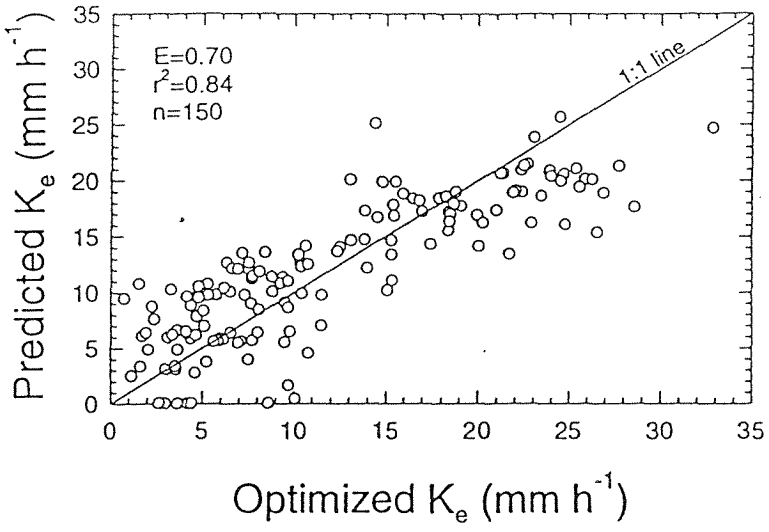

Figure 7.9.7. Comparison of WEPP optimized and predicted effective hydraulic conductivity for rangeland, K_{erange} ($mm \cdot h^{-1}$), using Eqs. [7.9.18] and [7.9.19]. E is the Nash-Sutcliffe coefficient of efficiency, r^2 is the coefficient of determination and n is the number of data points.

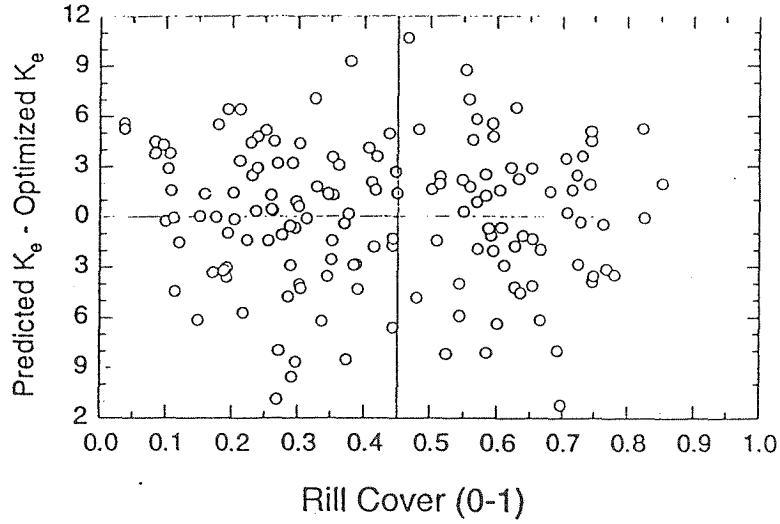

Figure 7.9.8. Differences between WEPP optimized and predicted K_{erange} using Eqs. [7.9.18] and [7.9.19].

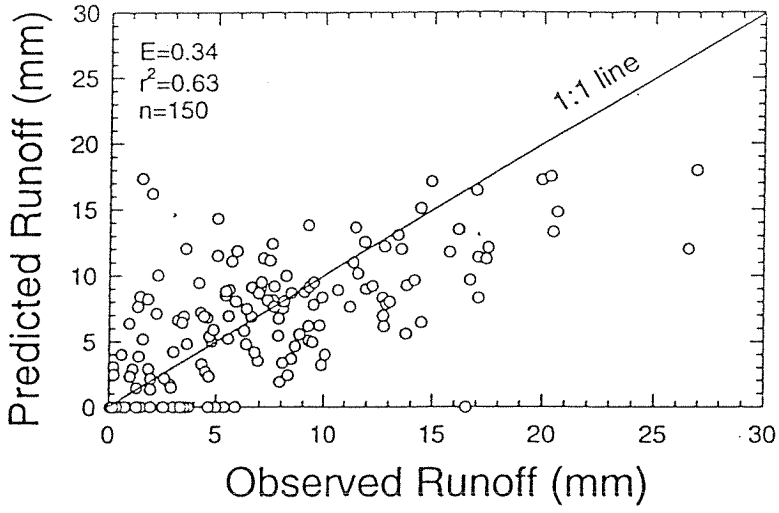

Figure 7.9.9. Comparison of WEPP predicted runoff using K_{erange} values estimated using Eqs. [7.9.18] and [7.9.19] and observed runoff. The data set of observed runoff is from the same plots that Eqs. [7.9.18] and [7.9.19] were developed. E is the Nash-Sutcliffe coefficient of efficiency, r^2 is the coefficient of determination and n is the number of data points.

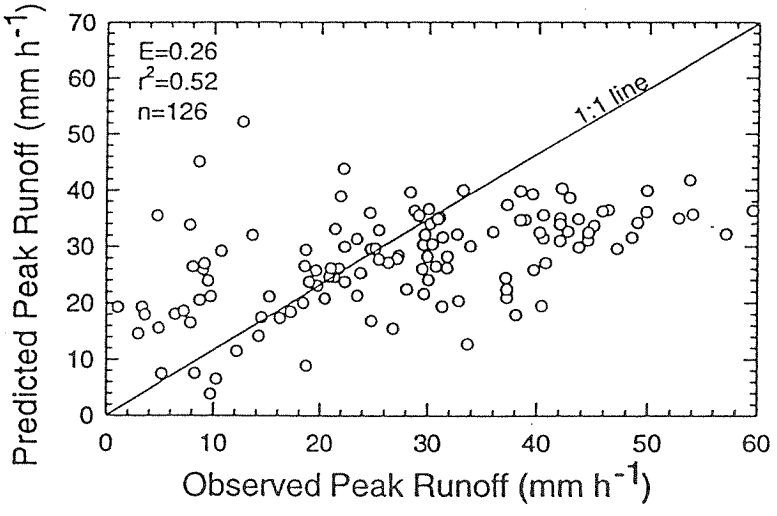

Figure 7.9.10. Comparison of WEPP predicted peak runoff using K_{erange} values estimated using Eqs. [7.9.18] and [7.9.19] and observed runoff. The data set of observed peak runoff is from the same plots that Eqs. [7.9.18] and [7.9.19] were developed. E is the Nash-Sutcliffe coefficient of efficiency, r^2 is the coefficient of determination and n is the number of data points. The number of data points shown is 126 because 24 plots had zero predicted runoff.

7.9.7 Freeze and Thaw Adjustments to Conductivity Values

The WEPP winter component (Chapter 3) computes frost and thaw development in the soil. When the soil is totally or partially frozen, an adjustment is made within the model to the hydraulic conductivity values used in the infiltration and percolation calculations.

The hydraulic conductivity adjustment for frozen soil (FS_a) is predicted from (Lee, 1983):

$$FS_a = 3.75\, e^{-0.26F_\theta} \qquad [7.9.20]$$

F_θ is predicted from:

$$F_\theta = \frac{\theta_f}{\theta_{fc}} 100 \qquad [7.9.21]$$

where θ_f is the volumetric soil water content at freezing ($m^3 \cdot m^{-3}$) and θ_{fc} is the volumetric soil water content at field capacity. If F_θ is greater than or equal to 100, FS_a is set equal to 0.1.

For the frozen soil layer, conductivity will be calculated using the equation

$$K_{frozen} = K_{unfrozen}(FS_a) \qquad [7.9.22]$$

where K_{frozen} represents the hydraulic conductivity that will be used for the frozen soil layer ($mm \cdot h^{-1}$), and $K_{unfrozen}$ is the hydraulic conductivity of the soil in an unfrozen condition ($mm \cdot h^{-1}$). If part of a soil layer is frozen, a weighted average (by frozen/unfrozen thickness) of the frozen and unfrozen conductivities is used for the infiltration and/or percolation computations.

7.10 Interrill Erodibility Parameters

7.10.1 Cropland Baseline Interrill Erodibility

The WEPP model is very sensitive to the input values for the soil erodibility parameters. The user must input a value for the baseline interrill erodibility (K_{ib}), which represents the erodibility of a freshly-tilled soil. If the user enters a value of 0.0 for K_{ib} in the soil input file, the baseline interrill erodibility for a cropland simulation will be set to 5,300,000 $kg \cdot s \cdot m^{-4}$.

A series of field experiments was conducted in 1987 and 1988 to develop estimation equations for erodibility parameters (Elliot et al., 1989). For cropland surface soils containing 30% or more sand, the equation for baseline interrill erodibility is:

$$K_{ib} = 2728000 + 19210000\ vfs \qquad [7.10.1]$$

where *vfs* is the fraction of very fine sand in the surface soil. If very fine sand content is greater than 0.40, use a maximum value of 0.40 in the equation.

For soils containing less than 30% sand, the equation is

$$K_{ib} = 6054000 - 5513000\ clay \qquad [7.10.2]$$

where *clay* is the fraction of clay in the surface soil. If clay content is less than 0.10, use 0.10 in the equation. Be sure to check the most recent version of the WEPP user summary document for any changes or updates to these equations. Table 7.10.1 provides suggested limits for K_{ib} values.

Table 7.10.1. Suggested limits for baseline values for K_i, K_r, and τ_c for cropland.

	K_{ib} $(kg \cdot s \cdot m^{-4})$	K_{rb} $(s \cdot m^{-1})$	τ_{cb} (Pa)
Minimum Value	500000	.002	0.3
Maximum Value	12000000	.050	7.0

7.10.2 Cropland Interrill Erodibility Adjustments

The baseline interrill erodibility on croplands is multiplied by an assortment of adjustment factors to account for various effects, including canopy cover, ground cover, roots, and sealing and crusting. The final adjusted interrill erodibility which is used on a day during a WEPP simulation is:

$$K_{iadj} = K_{ib}\,(CK_{ican})\,(CK_{igc})\,(CK_{idr})\,(CK_{ilr})\,(CK_{isc})\,(CK_{isl})\,(CK_{ifi}) \qquad [7.10.3]$$

where K_{iadj} is the adjusted interrill erodibility. The individual adjustment factors are described below.

7.10.2.1 Canopy Effects

The canopy adjustment factor, CK_{ican}, for K_{ib} is predicted from

$$CK_{ican} = 1 - 2.941\,\frac{cancov}{h}\left[1 - e^{-0.34h}\right] \qquad [7.10.4]$$

where h is the canopy height in meters.

7.10.2.2 Ground Cover

The ground cover adjustment factor (CK_{igc}) for K_i is predicted from

$$CK_{igc} = e^{-2.5\,inrcov} \qquad [7.10.5]$$

where *inrcov* is the interrill cover (0-1).

7.10.2.3 Roots

Effects of dead and live root biomass within the 0- to 0.15-m soil zone on interrill erodibility of a cropland soil are predicted separately. The effect of dead roots on interrill erodibility is predicted:

$$CK_{idr} = e^{-0.56\,dr} \qquad [7.10.6]$$

where CK_{idr} is the interrill erodibility adjustment for dead roots and dr is dead root mass $(kg \cdot m^{-2})$ within the 0- to 0.15-m soil zone.

The effect of live roots on interrill erodibility is predicted from:

$$CK_{ilr} = e^{-0.56\,lr} \qquad [7.10.7]$$

where CK_{ilr} is the interrill erodibility adjustment for live roots and lr is live root biomass $(kg \cdot m^{-2})$ within the 0- to 0.15-m soil zone.

There is no adjustment to account for the effect of buried residues on interrill erodibility.

7.10.2.4 Sealing and Crusting

The effect of sealing and crusting on interrill erodibility is predicted from:

$$CK_{isc} = \frac{K_{icons}}{K_{ib}} + \left[1 - \frac{K_{icons}}{K_{ib}}\right] e^{-\rho_c \, daydis} \qquad [7.10.8]$$

where CK_{isc} is the adjustment factor, K_{ib} is the baseline interrill erodibility, *daydis* is the cumulative number of days since total soil disturbance, and K_{icons} is the consolidated interrill erodibility and is calculated as:

$$K_{icons} = 10^3 \, (3042 - 3166 \, sand - 8816 \, orgmat - 2477 \, \theta_{cf}) \qquad [7.10.9]$$

7.10.2.5 Interrill Slope Adjustment

The interrill slope adjustment factor (CK_{isl}) is calculated as:

$$CK_{isl} = 1.05 - 0.85 \, e^{4 \sin\Omega} \qquad [7.10.10]$$

where Ω is the interrill slope angle. If the interrill slope angle is less than the average OFE slope, the average OFE slope is used in place of Ω in Eq. [7.10.10].

7.10.2.6 Freeze and Thaw

Soil that has undergone one or more freeze-thaw cycles is normally in a more erodible condition after thawing, at least until the soil dries. Adjustments to baseline interrill erodibility, rill erodibility, and critical shear stress are made from the time a frozen soil thaws until it dries to less than 1/3 bar water content. The adjustment equation is initially a function of the number of freeze-thaw cycles, until a maximum of 10 cycles have occurred during the current winter period.

$$CK_{ift} = acyc \; e^{-\ln\left[(acyc)\frac{\Psi_{surf}}{33}\right]} \qquad [7.10.11]$$

where CK_{ift} is the interrill adjustment factor due to freeze-thaw, Ψ_{surf} is the soil matric potential in the surface soil layer (*KPa*), and *acyc* is the freeze-thaw cycle factor. *acyc* is computed using:

$$acyc = 1 + 0.0586 \, (cycles) - 0.0027 \, (cycles)^2 \qquad [7.10.12]$$

where *cycles* is the number of freeze-thaw cycles in the current winter period. When *cycles* exceed 10, *acyc* is set to a constant 1.31.

7.10.3 Rangeland Baseline Interrill Erodibility

Data collected from a study of 18 rangeland sites (Simanton et al., 1987) in 1987 and 1988 were analyzed to develop a relationship between interrill erodibility and soil physical and chemical properties.

The baseline K_i is predicted from:

$$K_i = 1000 \, [\, 1810 - 1910 \, sand - 6327 \, orgmat - 846 \, \theta_{fc} \,] \qquad [7.10.13]$$

where K_i is the baseline interrill erodibility parameter for a rangeland soil ($kg \cdot s \cdot m^{-4}$), *sand* is the fraction of sand (0 to 1), *orgmat* is the fraction of organic matter (0 to 1), and θ_{fc} is the volumetric water content of the soil at 0.033 MPa ($m^3 \cdot m^{-3}$). If the predicted K_i is < 10,000 $kg \cdot s \cdot m^{-4}$, then K_i is set equal to 10,000. If K_i is > 2,000,000 $kg \cdot s \cdot m^{-4}$, then K_i is set equal to 2,000,000.

Table 7.10.2 gives the optimized erodibility values from the WEPP rangeland field studies. Table 7.10.3 gives the ranges of the variables used in developing Eq. [7.10.13]. It is recommended that Eq. [7.10.13] not be used with input data outside these ranges. Figure 7.10.1 compares the measured and predicted values of K_i. Table 7.10.4 lists the recommended upper and lower limits for rangeland K_i.

Table 7.10.2. Location and soil series description of mean site optimized interrill erodibility, K_i ($kg \cdot s \cdot m^{-4}$), rill erodibility, K_r ($s \cdot m^{-1}$), and critical shear stress, τ_c (Pa) from USDA rangeland rainfall simulation experiments.

Location[1]	Soil family	Soil series	Surface texture	Optimized K_i*	Optimized K_r*	Optimized τ_c
3) Tombstone, AZ	Ustochreptic calciorthid	Stronghold	Sandy loam	285	5.3	0.502
4) Tombstone, AZ	Ustollic haplargid	Forest	Sandy clay loam	263	3.5	1.306
5) Susanville, CA	Typic argixeroll	Jauriga	Sandy loam	270	1.2	0.313
10) Meeker, CO	Typic camborthid	Degater	Silty clay	1195	16.2	4.360
14) Sidney, MT	Typic argiboroll	Vida	Loam	315	3.2	0.025
17) Cuba, NM	Ustollic camborthid	Querencia	Sandy loam	445	1.7	0.576
18) Los Alamos, NM	Aridic haplustalf	Hackroy	Sandy loam	485	2.1	0.528
21) Chickasha, OK	Udic argiustoll	Grant	Loam[3]	357	1.5	1.160
22) Chickasha, OK	Udic argiustoll	Grant	Sandy loam	422	1.1	0.712
23) Freedom, OK	Typic ustochrept	Woodward	Loam	972	1.0	0.050
24) Woodward, OK	Typic ustochrept	Quinlan	Loam	469	8.3	1.880
25) Cottonwood, SD	Typic torrert	Pierre	Clay	1030	2.0	0.426
26) Cottonwood, SD	Typic torrert	Pierre	Clay	947	1.5	3.270
35) Mercury, NV	NA[4]	NA	Sandy loam	223	4.6	0.136
36) Mercury, NV	Thermic nadurargid	NA	Gravelly sandy loam	186	3.3	0.288
37) Ft. Supply, OK	Thermic haplustalf	Pratt	Sand	20	30.2	5.710
38) Freedom, OK	Thermic ustochrept	Woodward	Loam	903	0.9	0.001
39)Los Banos, CA	Thermic haploxeroll	Apollo	Loam	238	0.4	0.031

* K_i times 1,000 equals measured K_i. K_r divided by 10,000 equals measured K_r.

[1] Locations numbers in this table are consistant with location references in rangeland plant growth and effective hydraul ic conductivity (K_{erange}) tables and therefore are not numbered sequentially in this table. Locations 35 through 39 were used to develop soil erodibility coefficients for the WEPP model but were not used to develop K_{erange}.

[2] Farm land abandoned during the 1930's that had returned to rangeland. The majority of the 'A' horizon had been previously eroded.

[3] NA indicates data not available.

Table 7.10.3. Ranges of the variables used to develop Eq. [7.10.13].

Variable	Range	Units
sand	0.08 to 0.88	(*Fraction*)
orgmat	0.005 to 0.112	(*Fraction*)
θ_{fc}	0.04 to 0.40	($m^3 \cdot m^{-3}$)

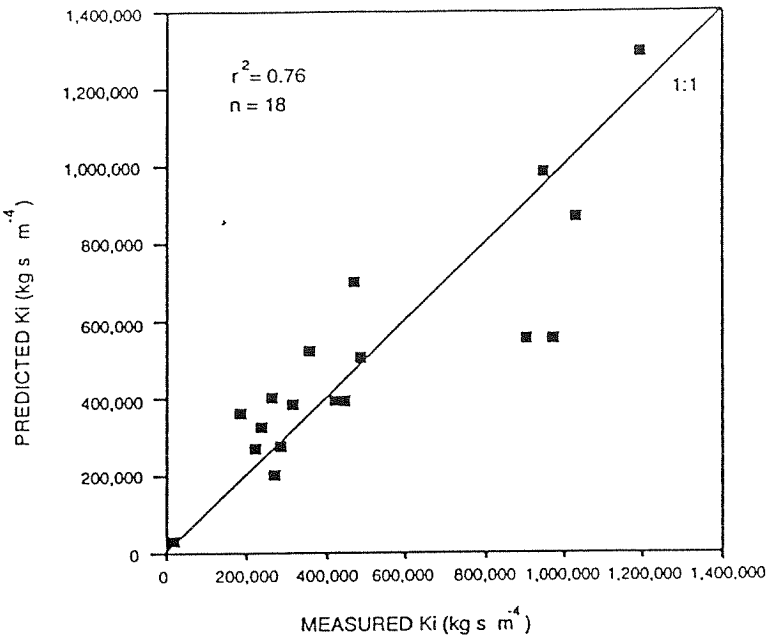

Figure 7.10.1. Rangeland measured vs. predicted K_i for eighteen WEPP field study sites.

Table 7.10.4. Suggested limits for predicted values for K_i, K_r, and τ_c for rangeland.

	K_i $(kg \cdot s \cdot m^{-4})$	K_r $(s \cdot m^{-1})$	τ_c *(pascals)*
Minimum Value	10000	0.00001	0.3
Maximum Value	2000000	0.004	7

7.10.4 Rangeland Interrill Erodibility Adjustments

Baseline interrill soil erodibility for rangelands is adjusted in a similar way to croplands, only there are currently less adjustment factors:

$$K_{iadj} = K_{ib}\ (RK_{icov})\ (RK_{ifl}) \qquad [7.10.14]$$

where K_{iadj} is the adjusted interrill erodibility, K_{ib} is the baseline interrill erodibility for the rangeland soil, RK_{icov} is the adjustment factor for rangeland cover, and RK_{ifl} is the adjustment for freezing and thawing.

7.10.4.1 Ground Cover Adjustment

The rangeland cover adjustment factor (RK_{icov}) for K_{ib} is predicted from:

$$RK_{icov} = e^{-7.0(inrcov + cancov)} \qquad [7.10.15]$$

where *inrcov* is the interrill cover (0-1) and *cancov* is the canopy cover (0-1).

7.10.4.2 Freeze and Thaw

Freeze and thaw adjustment relationships for cropland interrill erodibility, that are given in Eq. [7.10.11] are also applied to rangeland soils within a WEPP model simulation. Thus, $RK_{ifl} = CK_{ifl}$ in the WEPP model.

7.11 Rill Erodibility Parameters

7.11.1 Baseline Rill Erodibility and Critical Shear for Cropland Soils

The WEPP model is very sensitive to the input values for baseline rill erodibility and critical shear stress. Baseline erodibility parameters in cropland simulations are meant to represent the erodibility characteristics of a freshly-tilled soil. A baseline rill erodibility (K_{rb}) and a baseline critical hydraulic shear stress (τ_{cb}) must be supplied to the model in the soil input file by the user. If the user enters 0.0, the WEPP model sets the value of K_{rb} and τ_{cb} to 0.0115 $s \cdot m^{-1}$ and 3.1 *pascals*, respectively.

A set of field experiments conducted in 1987 and 1988 (Elliot et al., 1989). was used to derive the following equations, which can be used to estimate K_{rb} and τ_{cb}. For cropland surface soils containing 30% or more sand, the equations are:

$$K_{rb} = 0.00197 + 0.030\ vfs + 0.03863\ e^{-184\ orgmat} \qquad [7.11.1]$$

$$\tau_{cb} = 2.67 + 6.5\ clay - 5.8\ vfs \qquad [7.11.2]$$

where *vfs* is the fraction of very fine sand in the surface soil, *clay* is the fraction of clay in the surface soil, and *orgmat* is the fraction of organic matter in the surface soil. In the development of these equations, organic matter (*orgmat*) was assumed to be equal to 1.724 times the organic carbon content (*orgc*). If very fine sand content is less than 0.40, use 0.40 in the equations. If clay content is more than 0.40, use 0.40 in the equation. If organic matter content is less than 0.0035, use 0.0035 in the equation.

For cropland soils containing less than 30% sand,

$$K_{rb} = 0.0069 + 0.134\ e^{-20\ clay} \qquad [7.11.3]$$

$$\tau_{cb} = 3.5 \qquad [7.11.4]$$

If clay content is less than 0.10, use 0.10 in the equation.

Be sure to check the most recent WEPP user summary documentation for any changes or updates to these equations.

7.11.2 Cropland Rill Erodibility Adjustments

The baseline rill erodibility in the WEPP model is multiplied by a set of adjustment factors to account for various temporally-changing factors, including incorporated residue, roots, sealing and crusting, and freezing and thawing. The final adjusted rill erodibility for croplands which is used on a simulation day to predict rill detachment is:

$$K_{radj} = K_{rb}\ (CK_{rbr})\ (CK_{rdr})\ (CK_{rlr})\ (CK_{rsc})\ (CK_{rft}) \qquad [7.11.5]$$

where K_{radj} is the adjusted rill erodibility, K_{rb} is the baseline rill erodibility, and the other terms are the multiplicative adjustment factors described below.

7.11.2.1 Incorporated Residue

The following relationship is used to predict the effect of incorporated residue on K_r for a cropland soil

$$CK_{rbr} = e^{-0.4br} \quad [7.11.6]$$

where CK_{rbr} is the rill erodibility adjustment for buried residue and br is the mass of buried residue ($kg \cdot m^{-2}$) within the 0- to 0.15-m soil zone. This adjustment factor is based on the work of Alberts and Gantzer (1988) and Brown and Foster (1987).

7.11.2.2 Roots

The adjustments to K_r for dead roots (CK_{rdr}) and live roots (CK_{rlr}) are given as:

$$CK_{rdr} = e^{-2.2dr} \quad [7.11.7]$$

where dr is the mass of dead roots ($kg \cdot m^{-2}$)

$$CK_{rlr} = e^{-3.5lr} \quad [7.11.8]$$

where lr is mass of living roots ($kg \cdot m^{-2}$) within the 0- to 0.15-m soil zone.

7.11.2.3 Sealing and Crusting

The adjustment to K_r due to sealing and crusting (CK_{rsc}) is estimated by:

$$CK_{rsc} = \frac{K_{rcons}}{K_r} + \left(1 - \frac{K_{rcons}}{K_r}\right) e^{-\rho_c \, daydis} \quad [7.11.9]$$

where K_{rcons} is the consolidated rill erodibility and is predicted from:

$$K_{rcons} = 0.00035 - 0.0014\,\theta_{cf} + 0.00068\,silt + 0.0049\,M_{cf} \quad [7.11.10]$$

7.11.2.4 Freeze and Thaw

The adjustment for rill erodibility as the soil dries from saturation to field capacity is:

$$CK_{rft} = 2.0\,(0.933)^{\Psi_{surf}} \quad [7.11.11]$$

where Ψ_{surf} is the matric potential of the surface soil in KPa. Once the soil dries to field capacity, no further adjustment is made unless the soil surface becomes frozen then thaws once more.

7.11.3 Cropland Critical Hydraulic Shear Adjustments

As with the interrill and rill erodibilities, the baseline critical shear stress is multiplied by a set of adjustment factors to account for temporal variations in τ_c. The final adjusted τ_c value used on a day of simulation in the WEPP model is:

$$\tau_{cadj} = \tau_{cb}\,(C\tau_{rr})\,(C\tau_{sc})\,(C\tau_{cons})\,(C\tau_{ft}) \quad [7.11.12]$$

where τ_{cadj} is the adjusted critical shear stress value, τ_{cb} is the baseline critical shear stress value, and the multiplicative factors are as described below.

7.11.3.1 Random Roughness

The effect of random roughness on critical shear is calculated as:

$$C\tau_{rr} = 1.0 + 8.0\ (RR_t - 0.006) \qquad [7.11.13]$$

where RR_t is the random roughness of the surface soil (mm).

7.11.3.2 Sealing and Crusting

The adjustment to τ_c due to sealing and crusting ($C\tau_{sc}$) is predicted from:

$$C\tau_{sc} = \frac{\tau_{cons}}{\tau_c} + \left[1 - \frac{\tau_{cons}}{\tau_c}\right] e^{-\rho_c\ daydis} \qquad [7.11.14]$$

where τ_{cons} is the consolidated critical shear and is calculated as:

$$\tau_{cons} = 8.37 - 11.8\ \theta_{fc} - 4.9\ sand \qquad [7.11.15]$$

7.11.3.3 Freeze and Thaw

The adjustment to critical hydraulic shear stress for freezing and thawing effects is given by:

$$C\tau_{ft} = 0.875 + 0.0543\ \ln(\Psi_{surf}) \qquad [7.11.16]$$

where $C\tau_{ft}$ is the adjustment factor for critical shear stress and Ψ_{surf} is the matric potential of the surface soil (KPa). The adjustment becomes inactive once the soil becomes drier than field capacity (1/3 bar water content), and does not become active again until the soil has frozen and is thawing again.

7.11.4 Baseline Rill Erodibility and Critical Shear for Rangeland Soil

Data collected from a study of 18 rangeland soils (Simanton et al., 1987) conducted in 1987 and 1988 were analyzed to develop relationships between rill erodibility and critical shear stress and soil physical and chemical properties.

Baseline K_r for rangelands is predicted from:

$$K_r = 0.0017 + 0.0024\ clay - 0.0088\ orgmat - \frac{0.00088\ \rho_d}{1000} - 0.00048\ ROOT10 \qquad [7.11.17]$$

where K_r is the baseline rill erodibility for rangeland ($s \cdot m^{-1}$), $clay$ is soil clay content (0-1), $orgmat$ is organic matter content of the surface soil (0-1), ρ_d is dry soil bulk density ($kg \cdot m^{-3}$), and $ROOT10$ is total root mass in the top 10 cm of the soil surface ($kg \cdot m^{-2}$).

Table 7.11.1 gives the ranges of the variables used in developing Eq. [7.11.17]. It is recommended that Eq. [7.11.17] not be used with input data outside these ranges. The recommended lower and upper limits for rangeland K_r are given in Table 7.10.4.

Table 7.11.1. Ranges of the variables used to develop Eq. [7.11.17].

Variable	Range	Units
clay	0.033 to 0.422	*Fraction*
orgmat	0.005 to 0.112	*Fraction*
*ROOT*10	0.02 to 4.10	$kg \cdot m^{-2}$
ρ_d	1200 to 1800	$kg \cdot m^{-3}$

Critical shear stress can be predicted using:

$$\tau_c = 3.23 - 5.6\ sand - 24.4\ orgmat + \frac{0.9\rho_d}{1000} \quad [7.11.18]$$

where τ_c is the critical shear stress of the flow necessary to detach soil (Pa) and *sand* is the fraction of sand in the surface soil (0 to 1).

Table 7.11.2 gives the ranges of the variables used in developing Eq. [7.11.12]. It is recommended that Eq. [7.11.12] not be used with input data outside these ranges. The recommended lower and upper limits for rangeland τ_c are given in Table 7.10.3.

Table 7.11.2. Ranges of the variables used to develop Eq. [7.11.18].

Variable	Range	Units
sand	0.08 to 0.88	*Fraction*
orgmat	0.005 to 0.112	*Fraction*
ρ_d	1200 to 1800	$kg \cdot m^{-3}$

7.11.5 Rangeland K_r and τ_c Adjustments

Currently the only adjustment made to the baseline rangeland rill erodibility and critical shear stress parameters are due to soil freezing and thawing effects. The freeze and thaw adjustment relationships for cropland rill erodibility and critical shear given in Eqs. [7.11.11] and [7.11.16], respectively, are also applied in rangeland simulations in the WEPP model.

7.12 References

Alberts, E.E. and C.J. Gantzer. 1988. Influence of incorporated residue and soil consolidation on rill soil erodibility. Agronomy Abstracts. p. 270.

Bosch, D.D. and C.A. Onstad. 1988. Surface seal hydraulic conductivity as affected by rainfall. Trans. ASAE 31(4):1120-1127.

Brakensiek, D.L. and W.J. Rawls. 1983. Agricultural management effects on soil water processes Part II: Green and Ampt parameters for crusting soils. Trans. ASAE 26(6):1753-1759.

Brakensiek, D.L., W.J. Rawls and G.R. Stephenson. 1986. Determining the saturated hydraulic conductivity of soil containing rock fragments. Soil Sci. Soc. Am. J. 50(3):834-835.

Brown, L.C. and G.R. Foster. 1987. Rill erosion as affected by incorporated crop residue. ASAE Paper No. 87-2069, American Society of Agricultural Engineers, St. Joseph, MI.

Eigel, J.D. and I.D. Moore. 1983. Effect of rainfall energy on infiltration into a bare soil. In: Proc. of ASAE conference on Advances in Infiltration, Chicago, IL. pp.188-199.

Elliot, W.J., K.D. Kohl and J.M. Laflen. 1988. Methods of collecting WEPP soil erodibility data. ASAE Paper No. MCR 88-138, American Society of Agricultural Engineers, St. Joseph, MI.

Elliott, W.J., A.M. Liebenow, J.M. Laflen and K.D. Kohl. 1989. A Compendium of Soil Erodibility Data From WEPP Cropland Soil Field Erodibility Experiments 1987 & 1988. NSERL Report No. 3, USDA-ARS National Soil Erosion Research Lab., West Lafayette, IN.

Khan, M.J., E.J. Monke and G.R. Foster. 1988. Mulch cover and canopy effects on soil loss. Trans. ASAE 31(3):706-711.

Laflen, J.M., A.W. Thomas and R.W. Welch. 1987. Cropland Experiments for the WEPP project. ASAE Paper No. 87-2544, American Society of Agricultural Engineers, St. Joseph, MI.

Laws, J.O. 1941. Measurements of the fall-velocity of water-drop and raindrops. Trans. Am. Geophysical Union 22:706-721.

Lee, H.W. 1983. Determination of infiltration characteristics of a frozen Palouse silt loam soil under simulated rainfall. Ph.D. Dissertation, University of Idaho, Moscow, Idaho.

Onstad, C.A., M.L. Wolf, C.L. Larson and D.C. Slack. 1984. Tilled soil subsidence during repeated wetting. Trans. ASAE 27(3):733-736.

Potter, K.N. 1990. Soil properties effect on random roughness decay by rainfall. Trans. ASAE 33(6):1889-1892.

Rawls, W.J. and D.L. Brakensiek. 1983. A procedure to predict Green and Ampt infiltration parameters. Proc. of ASAE conference on Advances in Infiltration, Chicago, IL. pp.102-112.

Rawls, W.J., D.L. Brakensiek, J.R. Simanton and K.D. Kohl. 1990. Development of a Crust Factor for the Green Ampt Model. Trans. ASAE 33(4):1224-1228.

Risse, L.M. 1994. Validation of WEPP using Natural Runoff Plot Data. Unpubl. Ph.D. dissertation. National Soil Erosion Research Laboratory, Purdue University, West Lafayette IN. 230 pp.

Simanton, J.R., L.T. West, M.A. Weltz and G.D. Wingate. 1987. Rangeland experiment for the WEPP project. ASAE Paper No. 87-2545. American Society of Agricultural Engineers, St. Joseph, MI.

Van Doren, D.M. and R.R. Allmaras. 1978. Effect of Residue Management Practices on the soil physical environment, micro climate, and plant growth. Am. Soc. Agron. Spec. Publ. #31. Crop Residue Systems. ASA, CSSA, SSSA, Madison, WI. pp. 49-83.

Williams, J.R., C.A. Jones and P.T. Dyke. 1984. A modeling approach to determining the relationship between erosion and soil productivity. Trans. ASAE 27(1):129-142.

Wischmeier, W.H. 1966. Surface runoff in relation to physical and management factors. Proc. First Pan American Soil Conservation Congress. San Paulo, Brazil. p. 237-244.

7.13 List of Symbols

Symbol	Definition	Units	Variable
acyc	Freeze-thaw cycle factor	-	acyc
b	Adjustment coefficient for random roughness	-	crr
BASCOV	Total basal surface cover fraction (0-1)	*Fraction*	bascov
BASI	Fraction of basal surface cover in interrill areas	*Fraction*	basi
BASR	Fraction of basal surface cover in rill areas	*Fraction*	basr
br	Mass of buried residue within the 0- to 0.15 m soil zone	$kg \cdot m^{-2}$	smrm
c	Coefficient relating amount of kinetic energy since last tillage to the speed of crust formation	$m^2 \cdot J^{-1}$	cke
cancov	canopy cover	*Fraction*	cancov
C_{br}	Random roughness and ridge height adjustment factor for buried residue	*Fraction*	cbr
ccovef	Effective canopy cover	*Fraction*	ccovef
CEC	Cation exchange capacity	*meq*/100*g*	cec
CEC_c	Cation exchange capacity of clay	*meq*/100*g*	cecc
CEC_r	$CEC_c/clay$	*meq*/100*g*	solcon
CF	Crust factor	*Fraction*	crust
C_h	Hydraulic conductivity adjustment factor for canopy height	*Fraction*	-
CK_{ican}	Cropland interrill erodibility adjustment factor for canopy cover	*Fraction*	ckiacc
CK_{idr}	Cropland interrill erodibility adjustment factor for dead root	*Fraction*	ckiadr
CK_{ift}	Cropland interrill erodibility adjustment factor for freeze and thaw	*Fraction*	ckiaft
CK_{igc}	Cropland interrill erodibility adjustment factor for ground cover	*Fraction*	ckiagc
CK_{ilr}	Cropland interrill erodibility adjustment factor for live roots	*Fraction*	ckialr
CK_{isc}	Cropland interrill erodibility adjustment factor for sealing and crusting	*Fraction*	ckiasc
CK_{isl}	Cropland interrill erodibility adjustment factor for slope	*Fraction*	ckiasl
CK_{rbr}	Cropland interrill erodibility adjustment factor for residue	*Fraction*	ckiabr
CK_{rdr}	Cropland interrill erodibility adjustment factor for dead roots	*Fraction*	ckiadr
CK_{rft}	Cropland rill erodibility adjustment factor for freeze and thaw	*Fraction*	ckraft
CK_{rlr}	Cropland rill erodibility adjustment factor for live roots	*Fraction*	ckalr
CK_{rsc}	Cropland interrill erodibility adjustment factor for sealing and crusting	*Fraction*	ckrasc
clay	Clay content of the soil	*Fraction*	clay
CN	Curve number	-	-
$C\tau_{ft}$	Critical shear adjustment factor for freeze and thaw	*Fraction*	tcaft
$C\tau_{rr}$	Critical shear adjustment factor for random roughness	*Fraction*	tcarr
$C\tau_{sc}$	Critical shear adjustment factor for sealing and crusting	*Fraction*	tcasc
cycles	Number of freeze-thaw cycles in current winter period	-	cycle
daycnt	Counter to track the number of days since the last tillage operation	*d*	daycnt
daydis	The number of days since disturbance	*d*	daydis
D_g	Depth of the soil horizon of interest	*m*	dg
dr	Amount of dead root mass	$kg \cdot m^{-2}$	rtm
E_a	Cumulative kinetic energy of the rainfall since the last tillage operation	$J \cdot m^{-2}$	rkecum
F_a	Volume of entrapped air in the soil	*Fraction*	coca
F_{cf}	Correction for the volume of coarse fragment in the soil	*Fraction*	cpm
F_{dc}	Daily soil bulk density consolidation factor	*Fraction*	daycon
F_θ	Ratio of soil water content at freezing to to the soil water content at field capacity	%	-
FS_a	Hydraulic conductivity adjustment for frozen soil	*Fraction*	frof
FBASI	Basal surface cover area fraction on the interrill areas	*Fraction*	fbasi
FBASR	Basal surface cover area fraction in the rill channels	*Fraction*	fbasr

FRESI	Residue cover area fraction on interrill areas	*Fraction*	fresi
FRESR	Residue cover area fraction in the rill channels	*Fraction*	fresr
h	Canopy height	m	canhgt
inrcov	Interrill cover	*Fraction*	inrcov
K_{appr}	Approximation of hydraulic conductivity for each event under meadow condition	$mm \cdot h^{-1}$	-
K_b	Baseline effective hydraulic conductivity	$mm \cdot h^{-1}$	avks
K_{bare}	Effective K_b after adjustment for crusting and tillage	$mm \cdot h^{-1}$	kbare
K_e	Effective hydraulic conductivity in fill layer	$mm \cdot h^{-1}$	eke
K_{ec}	Time-invariant effective hydraulic condutivity	$mm \cdot h^{-1}$	-
K_{ef}	Effective hydraulic conductivity for fallow soil conditions	$mm \cdot h^{-1}$	-
K_{erange}	Effective hydraulic conductivity for rangeland soils	$mm \cdot h^{-1}$	-
K_i	Interrill soil erodibility	$kg \cdot s \cdot m^{-4}$	-
K_{iadj}	Adjusted interrill soil erodibility	$kg \cdot s \cdot m^{-4}$	kiadjf*ki
K_{ib}	Baseline interrill soil erodibility	$kg \cdot s \cdot m^{-4}$	ki
K_{icons}	Consolidated interrill soil erodibility	$kg \cdot s \cdot m^{-4}$	kconsd
K_r	Rill soil erodibility	$s \cdot m^{-1}$	-
K_{radj}	Adjusted rill soil erodibility	$s \cdot m^{-1}$	kradjf*kr
K_{rb}	Baseline rill soil erodibility	$s \cdot m^{-1}$	kr
K_{rcons}	Consolidated rill soil erodibility	$s \cdot m^{-1}$	kconsd
$K_{unfrozen}$	Hydraulic conductivity of soil in unfrozen condition	$mm \cdot h^{-1}$	sscunf
K_{frozen}	Hydraulic conductivity of soil in frozen condition	$mm \cdot h^{-1}$	-
L	Depth of wetting front	m	wetfrt
lr	Amount of live root mass	$kg \cdot m^{-2}$	rtm15
M_{cf}	Coarse fragment content by weight	*Fraction*	rfg
ME	Nash-Sutcliffe model efficiency	-	-
Ω	Interrill slope angle	*rad*	-
orgc	Organic carbon content	*Fraction*	orgc
orgmat	Organic matter content	*Fraction*	orgmat
ϕ_e	Effective porosity	*Fraction*	epor
ϕ_t	Total porosity	*Fraction*	por
ρ_c	Consolidated soil bulk density at 0.033 *MPa*	$kg \cdot m^{-3}$	bdcons
$\Delta\rho_c$	Difference in bulk density between a soil that is naturally consolidated and one that has received 0.1 m of rainfall	$kg \cdot m^{-3}$	bddiff
ρ_d	Soil bulk density at the wilting point	$kg \cdot m^{-3}$	bddry
$\Delta\rho_{mx}$	Maximum increase in soil bulk density with rainfall	$kg \cdot m^{-3}$	A_o
$\Delta\rho_{rf}$	Adjustment for increasing bulk density due to consolidation by rainfall	$kg \cdot m^{-3}$	bdrif
ρ_t	Soil bulk density after tillage	$kg \cdot m^{-3}$	bdtill
$\Delta\rho_{wt}$	Daily increase in soil bulk density after 0.1 m of rainfall	$kg \cdot m^{-3}$	bdiwt
ρ_b	Bulk density	$kg \cdot m^{-3}$	bd
rain	Storm rainfall amount	*mm*	rain
RESI	Fraction of litter surface cover on interrill areas	*Fraction*	resi
RK_{icov}	Interrill erodibility adjustment factor for rangeland cover	*Fraction*	rkiagc
RK_{ift}	Interrill erodibility adjustment for freezing and thawing	*Fraction*	rkiaft
R_c	Cumulative rainfall since tillage	m	rfcum
rescov	Residue cover	*Fraction*	rescov
RH_o	Ridge height immediately after tillage	m	rho
RH_t	Ridge height at time t	m	rh
*ROOT*10	Total live and dead root mass in the top 0.1 m of soil	$kg \cdot m^{-2}$	rooty
RR	Random roughness of the soil	m	-
RR_t	Random roughness at time t	m	rrc

RR_i	Random roughness immediately after tillage	*m*	rrinit
RR_o	Random roughness of a tillage implement	*m*	rro
sand	sand content	*Fraction*	sand
SC	Correction factor for partial saturation of the subcrust soils	*Fraction*	sc
scovef	Total effective surface cover	*Fraction*	scovef
silt	Silt content	*Fraction*	silt
T_{ds}	Fraction of the soil surface disturbed by a tillage implement	*Fraction*	surdis
τ	Shear stress of the flow	*Pa*	tau
τ_c	Critical shear stress of the flow necessary to initiate detachment	*Pa*	-
τ_{cadj}	Adjusted critical shear stress	*Pa*	tcadjf*shcrit
τ_{cb}	Baseline critical shear stress	*Pa*	shcrit
τ_{cons}	Consolidated critical shear stress	*Pa*	kconsd
θ	Soil water content by volume	*Fraction*	thet
θ_d	Soil water content at 1.5 MPa by volume	*Fraction*	thetdr
θ_f	Soil water content at freezing by volume	*Fraction*	smf
θ_{fc}	Soil water content at 0.033 MPa by volume	*Fraction*	thetfc
θ_r	Residual water content by volume	*Fraction*	wrd
V_{cf}	Coarse fragment content by volume	*Fraction*	vcf
vfs	Fracton of very fine sand in surface soil	*Fraction*	-
Ψ	Steady state capillary potential at the crust/subcrust interface	-	ffi
Ψ_{surf}	Soil matric potential in the surface soil layer	*KPa*	tenkpa